Searches for Higgs boson pair production with the full LHC Run 2 dataset in ATLAS

Sean Gasiorowski (on behalf of ATLAS)
University of Washington

Phenomenology Symposium
24th – 26th May 2021

ATLAS EXPERIMENT

Introduction

- Higgs boson pair production ("di-Higgs") an active topic at the LHC!
- A huge amount of searches published with early Run-2 data
- ATLAS experiment:
    - Early Run 2: 36 fb^{-1}
    - Full Run 2: 139 fb^{-1}
- Now have ~4x the data – even more opportunity for exciting results!

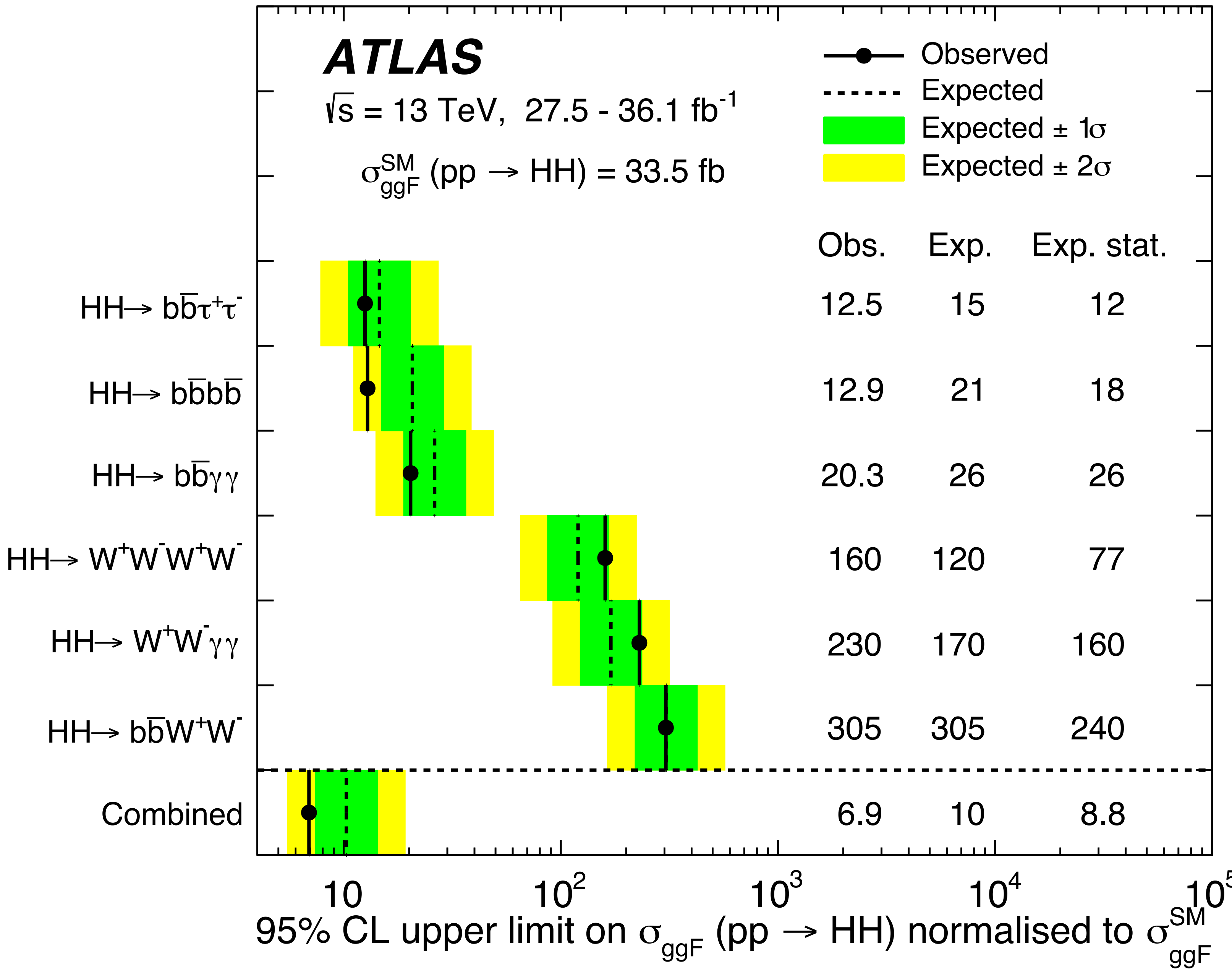

Combined HH results (early Run 2)
Phys. Lett. B 800 (2020) 135103

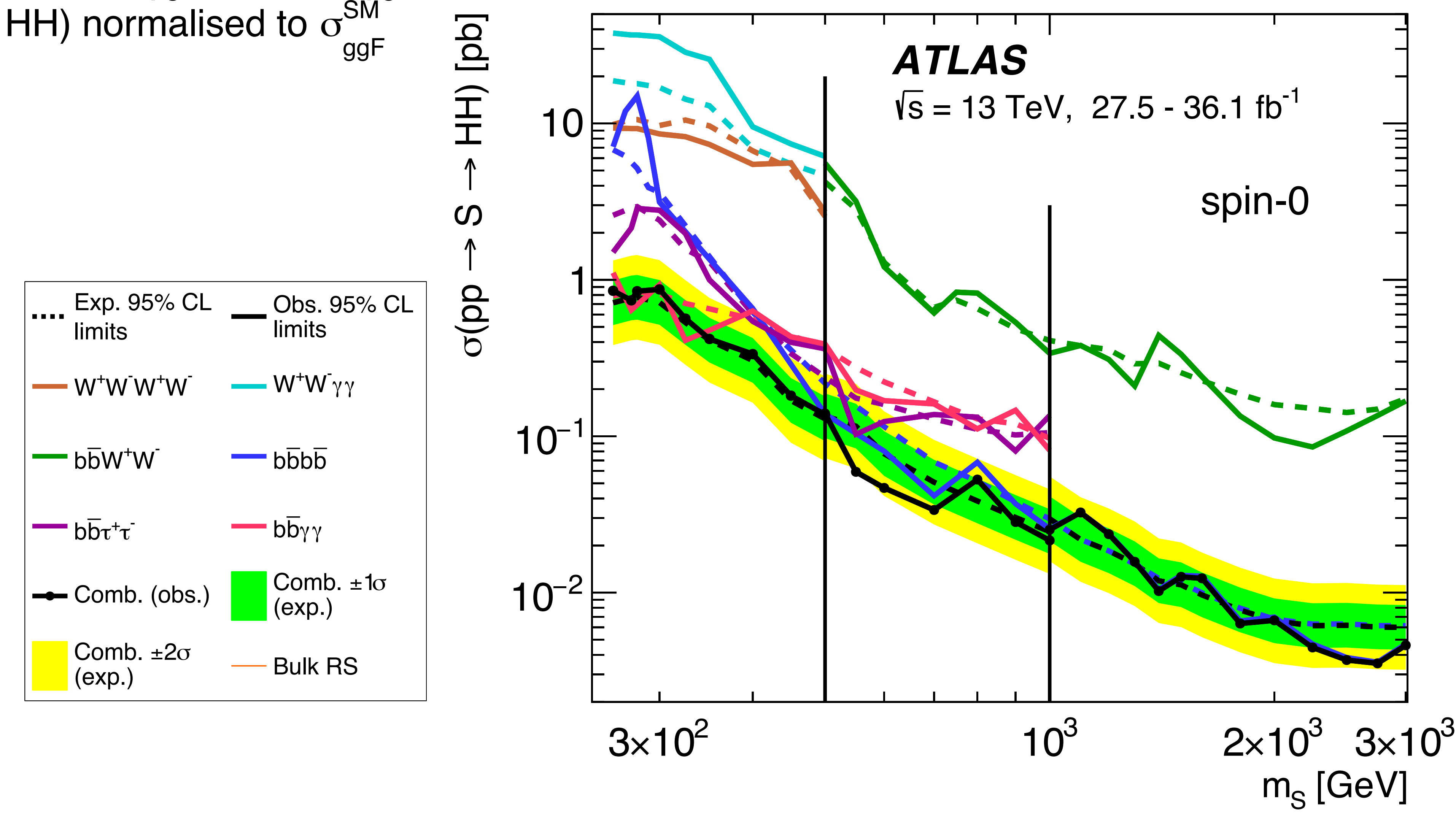

Introduction: Searches for HH

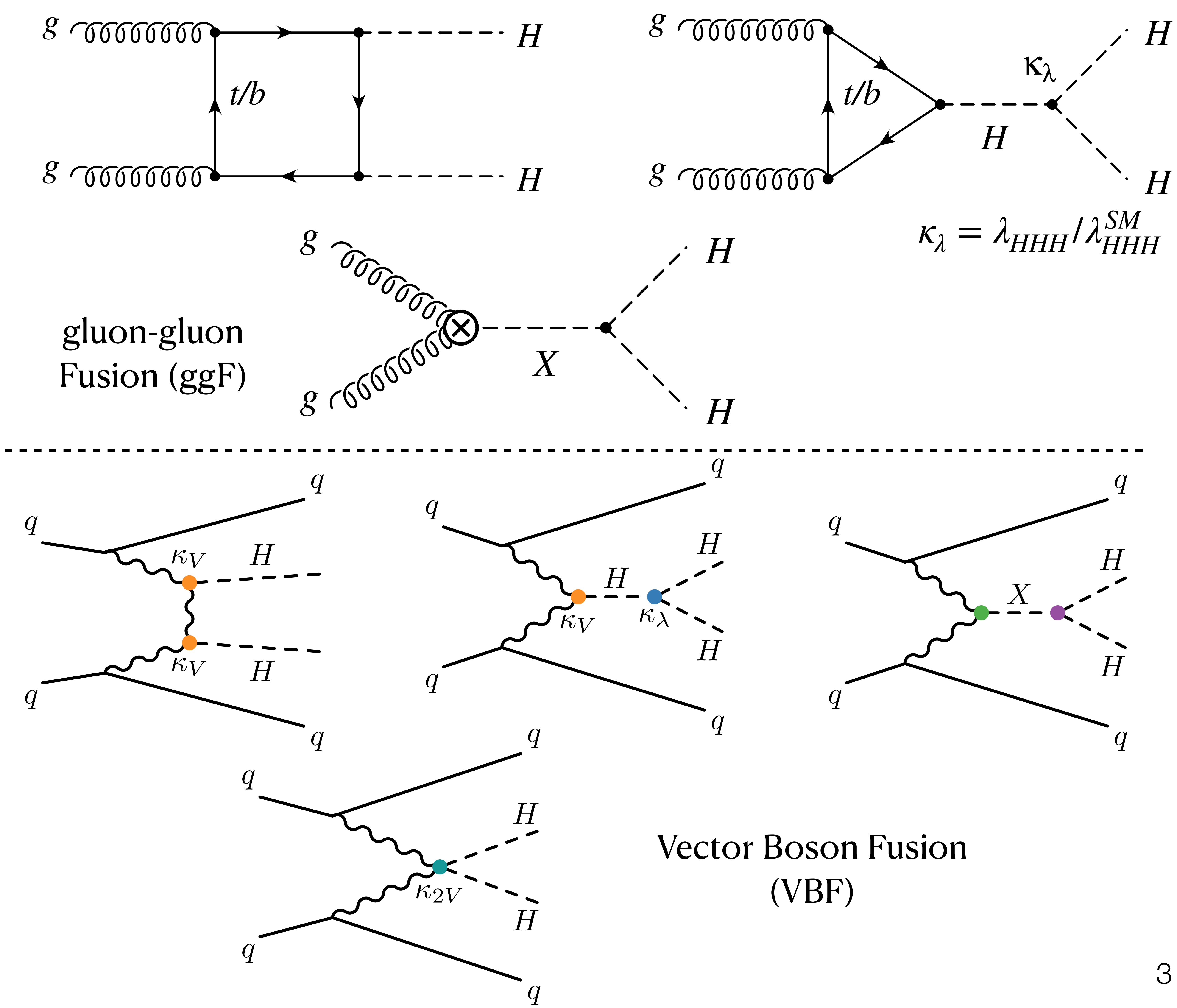

- Discovery of the Higgs boson by ATLAS and CMS opens up many new avenues for searches
- Non-resonant HH production is sensitive to the Higgs **self-coupling** (Standard Model parameter!)
- A large variety of Beyond the Standard Model **resonances** can decay to HH
  - e.g. heavy scalar from two Higgs doublet models [arXiv:1106.0034]
- Theoretical ggF HH cross section: 31.05 fb at $\sqrt{s}$ = 13 TeV [LHC-HH WG]
- Theoretical VBF HH cross section: 1.726 fb at $\sqrt{s}$ = 13 TeV [LHC-HH WG]
- Context: ggF single Higgs 46.86 **pb** [LHC-H WG]

Introduction: Searches for HH

- Dominant branching fraction of Standard Model Higgs is to $b\bar{b}$ (~58%) => HH channels often have one $H \to b\bar{b}$, one $H \to$ something else
- Results today:
  - Context: Early Run 2 $HH \to b\bar{b}\tau^+\tau^-$
  - Full Run 2 ATLAS results for four HH channels:
    - Boosted $HH \to b\bar{b}\tau^+\tau^-$ (hadronic)
    - VBF $HH \to b\bar{b}b\bar{b}$
    - $HH \to b\bar{b}\ell\nu\ell\nu$
    - $HH \to b\bar{b}\gamma\gamma$
  - HL-LHC prospects (based on early Run 2 results)

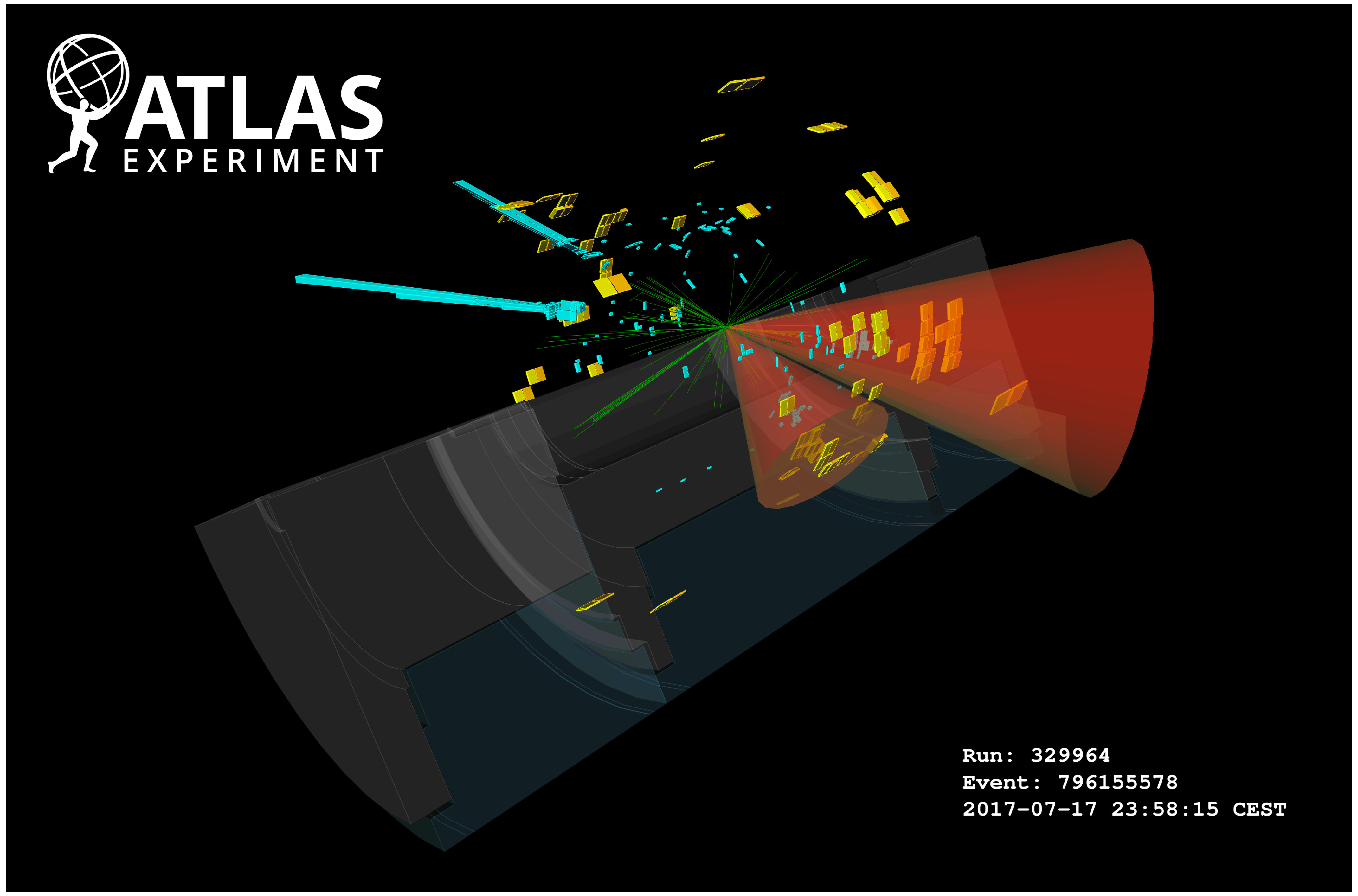

Candidate $HH \to b\bar{b}\gamma\gamma$ event (from ATLAS-CONF-2021-016)

$HH \to b\bar{b}\tau^+\tau^-$: Early Run 2

- Early Run 2 searches:
  - Small radius jets (R=0.4) jets used to reconstruct the visible component of hadronic τ lepton decay ("resolved")
  - For signals with high resonance masses, H decay products very collimated (high Lorentz boost) => overlapping τ's
- Analysis restricted to lower resonance masses (< 1 TeV)
  - Search also includes non-resonant HH, with observed (expected) limits of 30.9 fb (36.1 fb), 12.7 (14.8) times the SM prediction

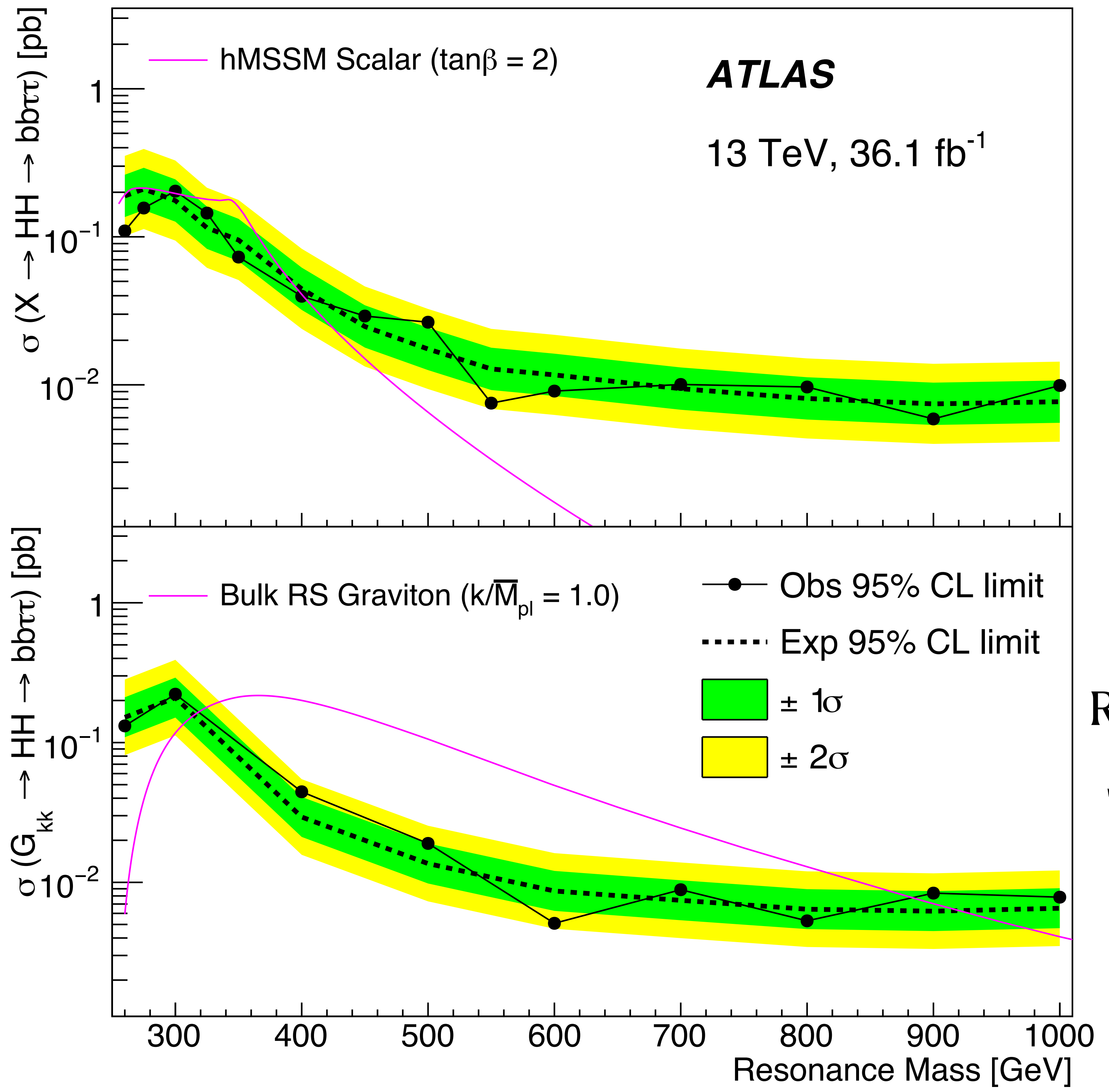

hMSSM:
305 GeV < m_X < 402 GeV
excluded at 95% CL

Randall Sundrum Graviton:
325 GeV < m_{GKK} < 885 GeV
excluded at 95% CL

		Observed	-1σ	Expected	$+1\sigma$
$\tau_{lep}\tau_{had}$	$\sigma(HH \to bb\tau\tau)$ [fb]	57	49.9	69	96
	σ/σ_{SM}	23.5	20.5	28.4	39.5
$\tau_{had}\tau_{had}$	$\sigma(HH \to bb\tau\tau)$ [fb]	40.0	30.6	42.4	59
	σ/σ_{SM}	16.4	12.5	17.4	24.2
Combination	$\sigma(HH \to bb\tau\tau)$ [fb]	30.9	26.0	36.1	50
	σ/σ_{SM}	12.7	10.7	14.8	20.6

Phys.Rev.Lett. 121 (2018) 19, 191801

Boosted $HH \to b\bar{b}\tau^+\tau^-$

- New! Consider boosted di-τ object: large radius (R=1.0) jet with τ's identified with R=0.2 subjets

- Extends di-τ reconstruction efficiency to lower ΔR

- First time such an approach used in ATLAS!

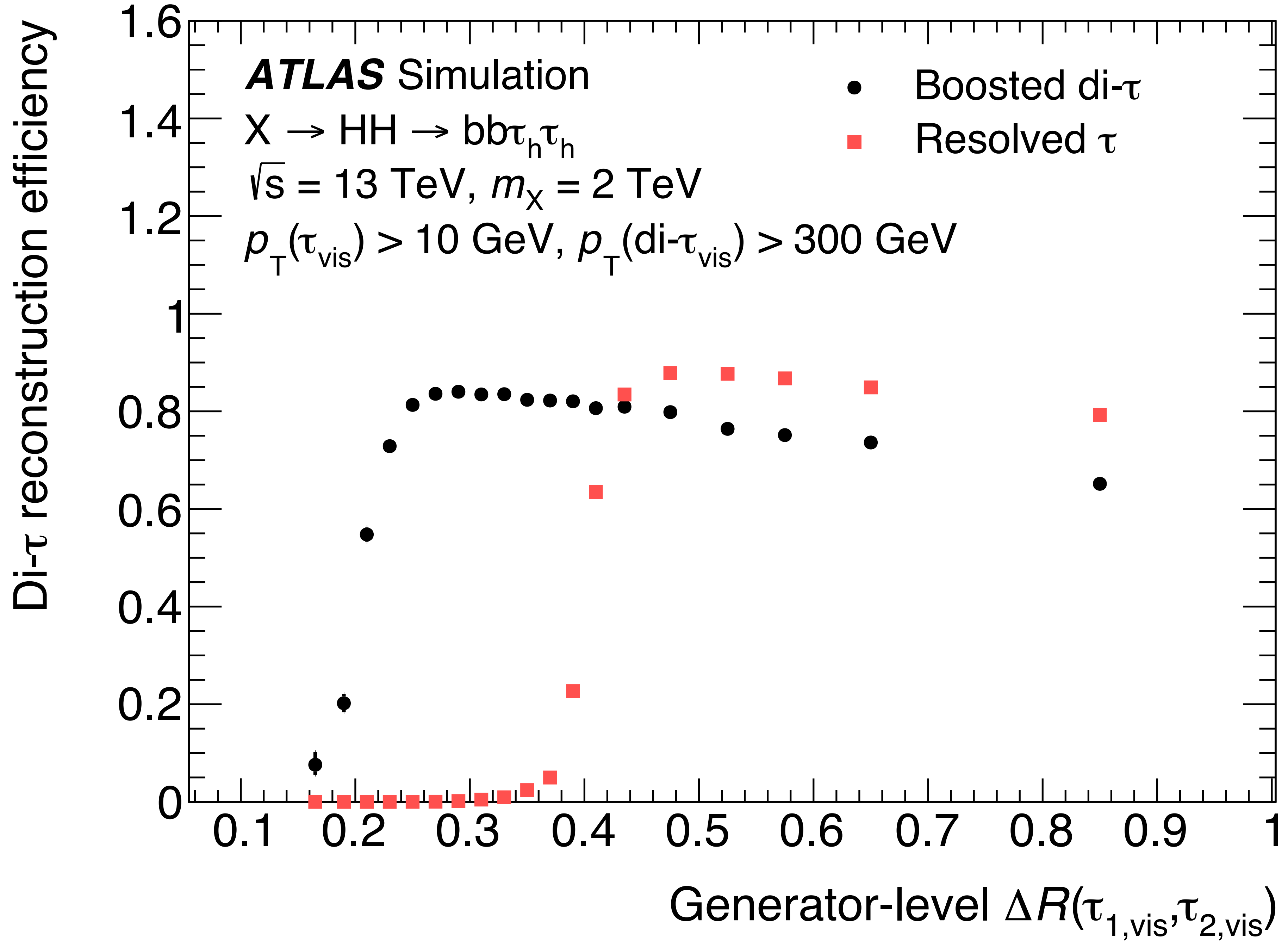

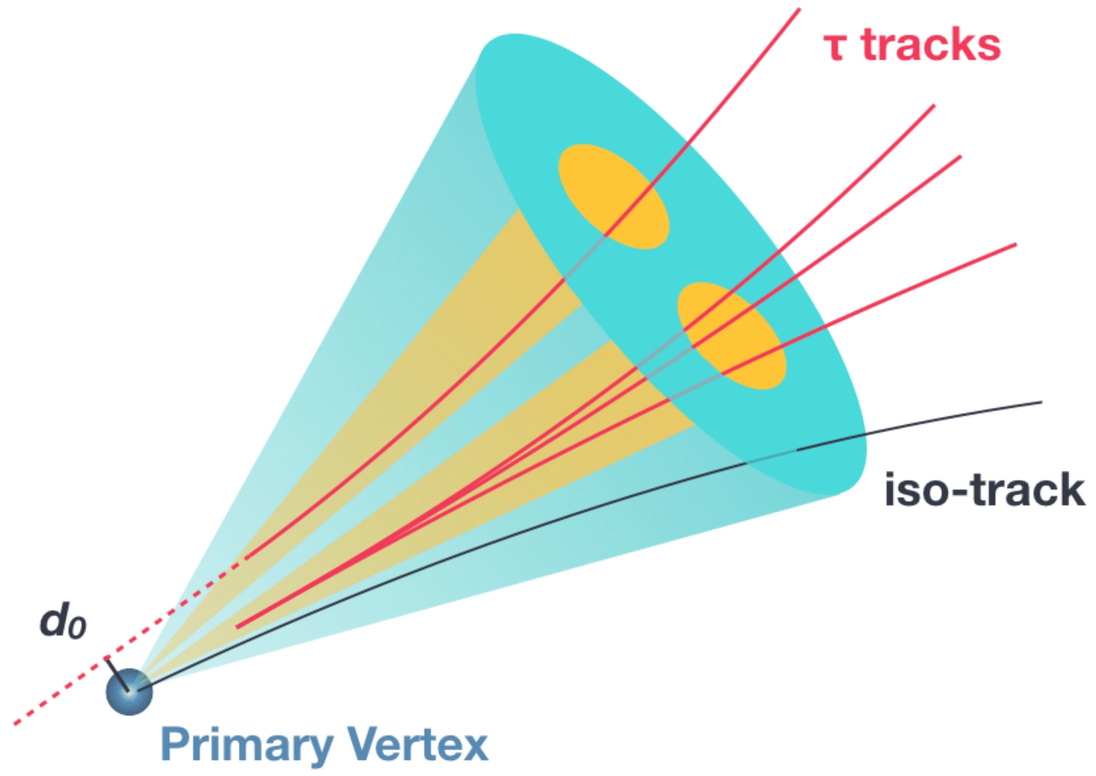

JHEP11(2020)163

Boosted $HH \rightarrow b\bar{b}\tau^+\tau^-$

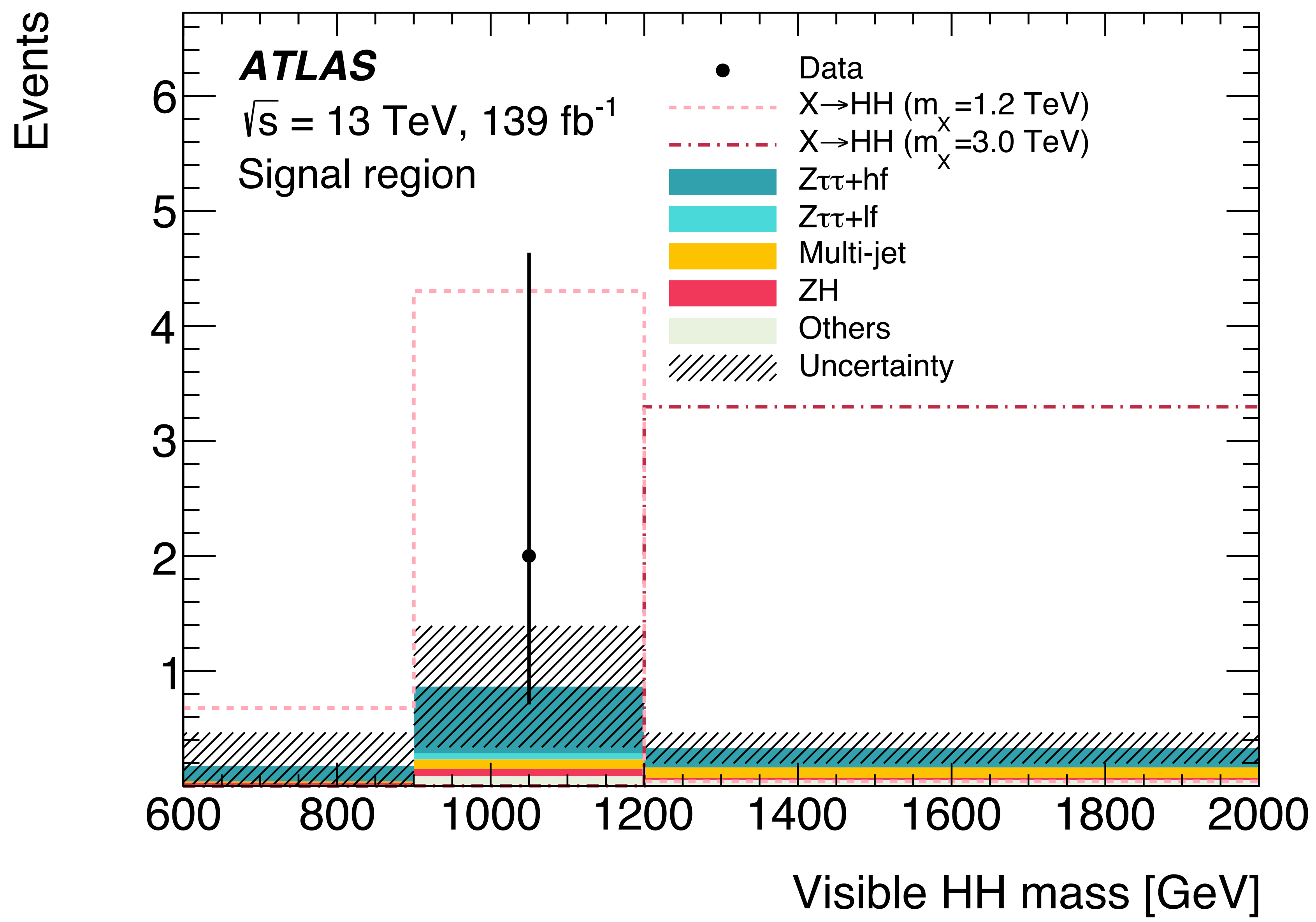

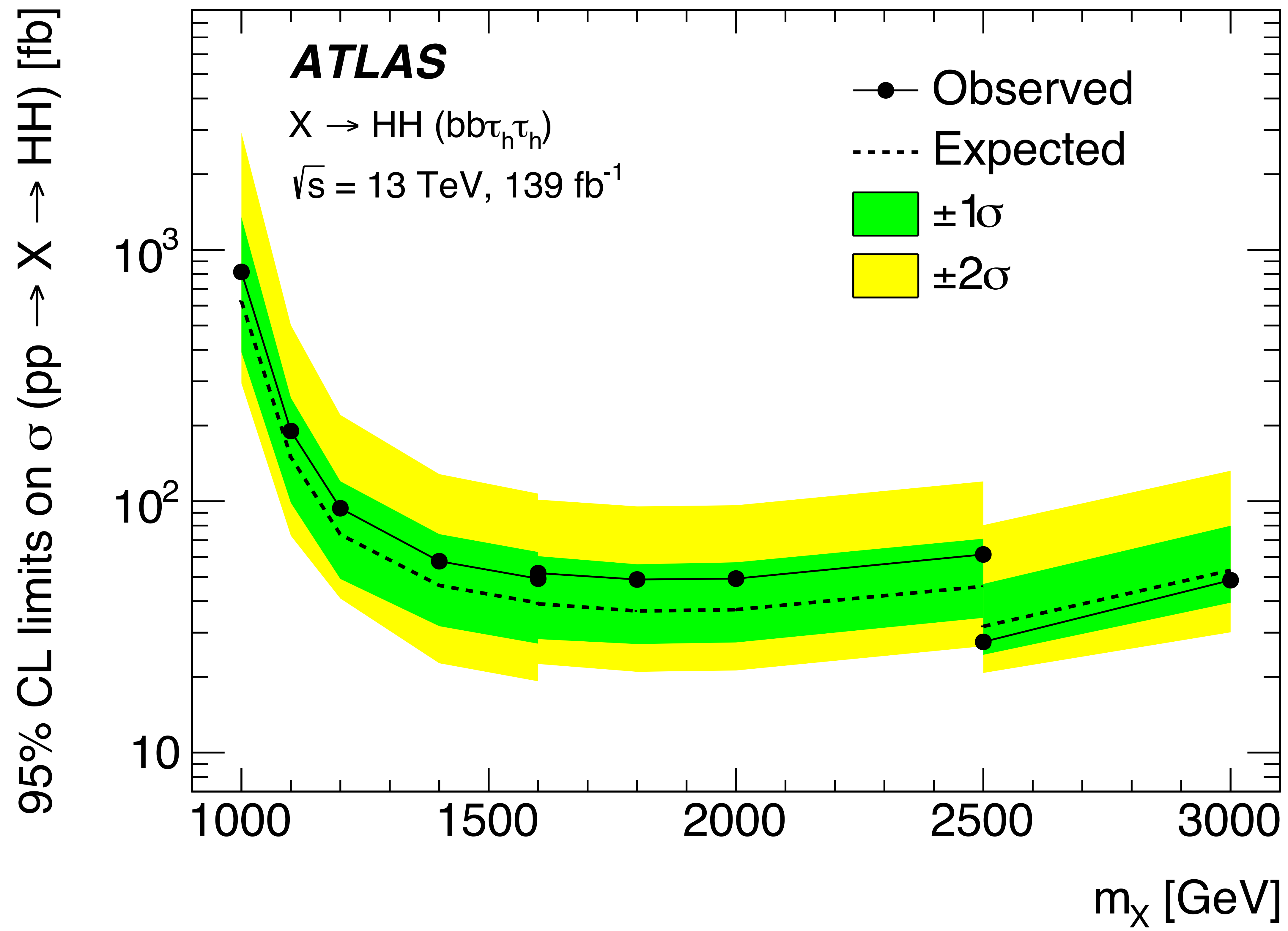

- Boosted di-τ tagger used for di-τ reconstruction
- BDT used to distinguish from quark/gluon initiated jets (input variables in backup)
- Limits set using single bin counting experiments for resonances from 1 to 3 TeV. No significant excesses observed.

Note: discontinuities in limits come from resonance mass-dependent cuts on m_{HH}^{vis}

$m_{HH}^{vis} > 0$ GeV if $m_X < 1.6$ TeV,
$m_{HH}^{vis} > 900$ GeV $m_X \geq 1.6$
$m_{HH}^{vis} > 1200$ GeV if $m_X \geq 2.5$ TeV

JHEP11(2020)163

VBF $HH \rightarrow b\bar{b}b\bar{b}$

- HH produced via vector boson fusion, decaying to $b\bar{b}b\bar{b}$
  - First time this search has been done in ATLAS!
- Analysis strategy builds off of early Run 2 gluon-gluon fusion result, with refinements for VBF
- Selection: variety of kinematic cuts (see backup for more details)
- Data driven reweighting used for multijet background estimation

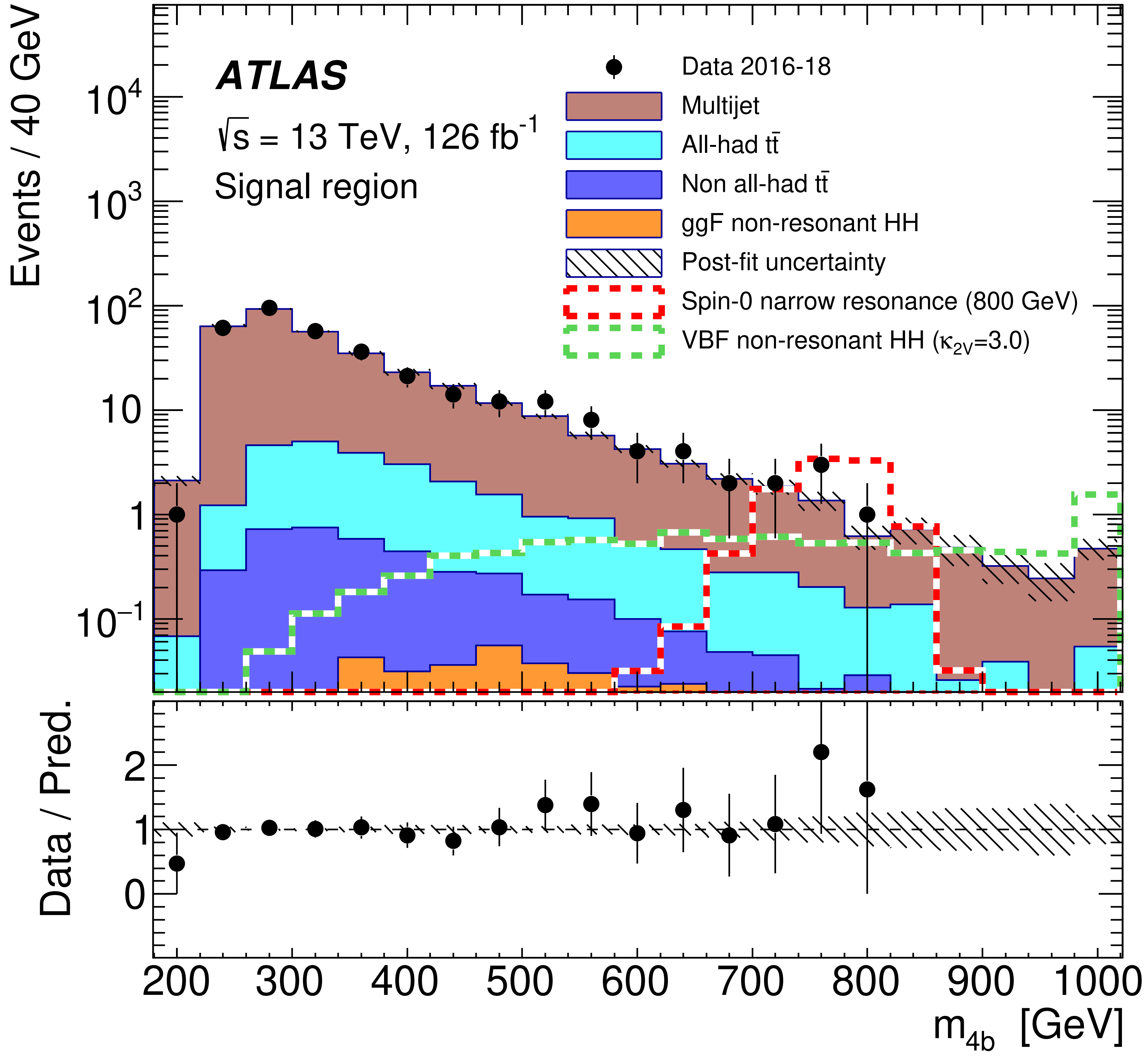

Note: 126 fb-1 of data used for this analysis (vs. 139 fb-1) due to (1) a trigger inefficiency in 2016 data taking and (2) the choice to not include 2015 due to large differences in the b-jet trigger menu

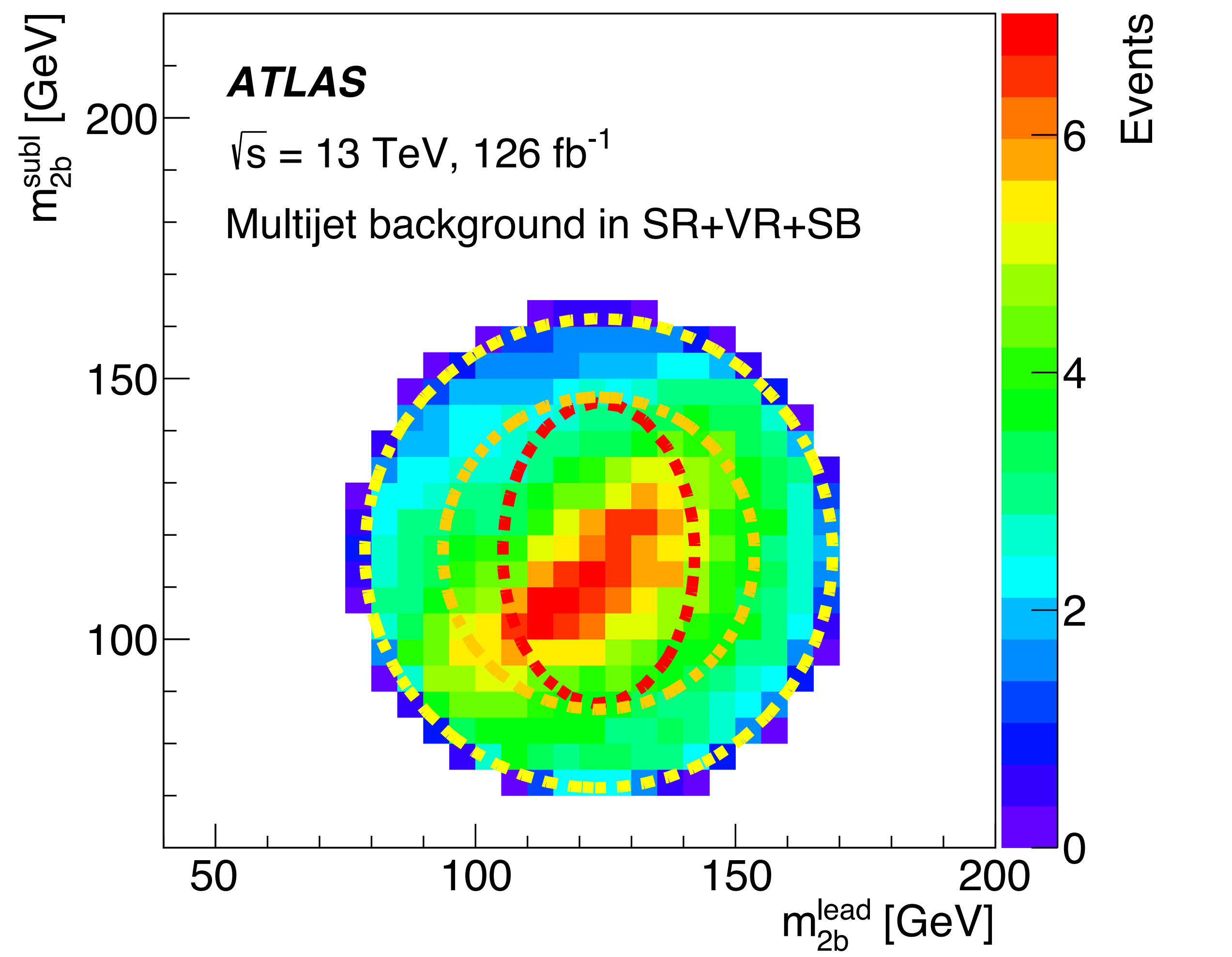

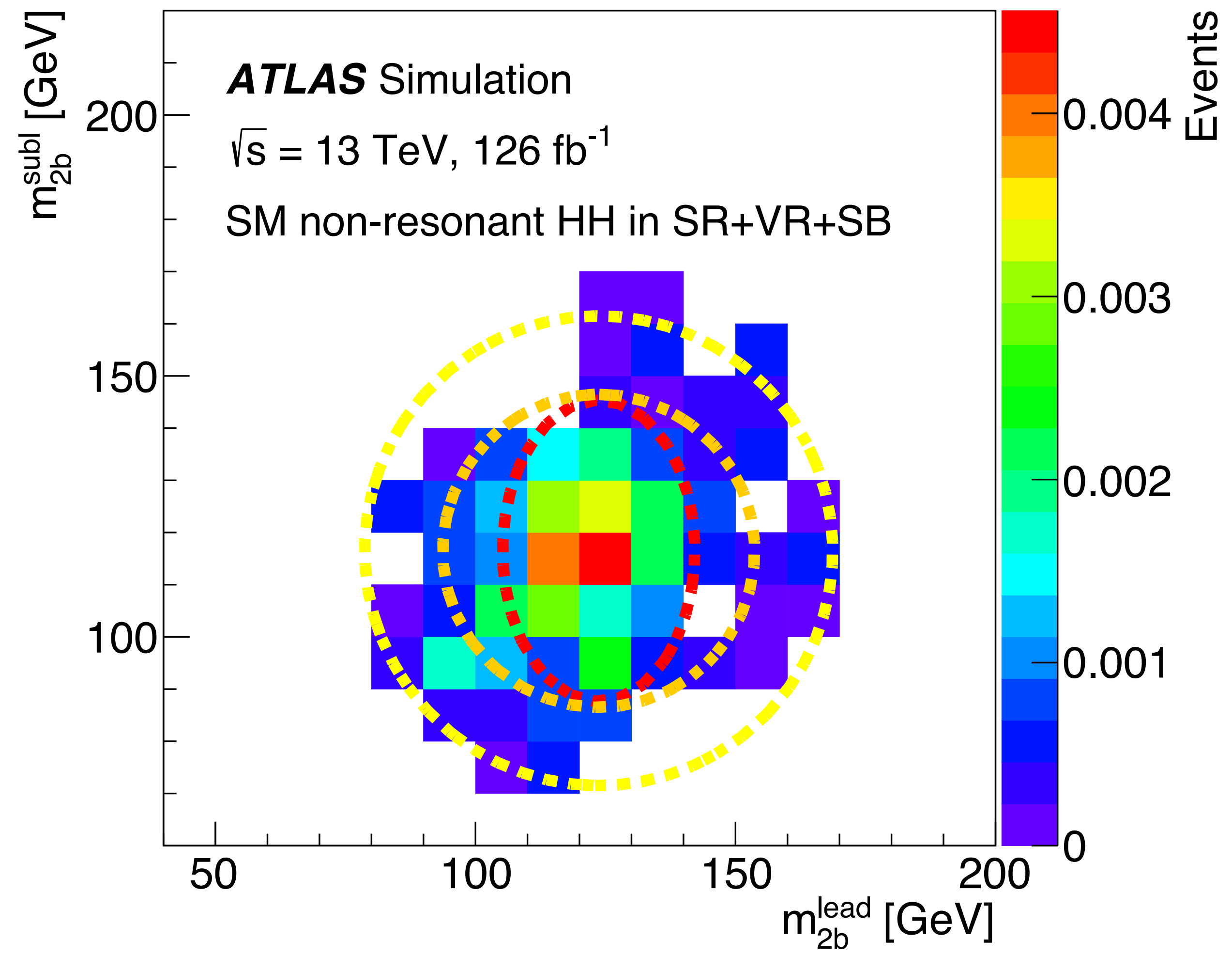

JHEP07(2020)108

VBF $HH \to b\bar{b}b\bar{b}$

- No significant excesses observed
- Limits set on:
  - Scalar resonances (narrow and broad width)
  - SM non-resonant production
  - Variations of coupling of coupling of HH to two vector bosons (κ_{2V})

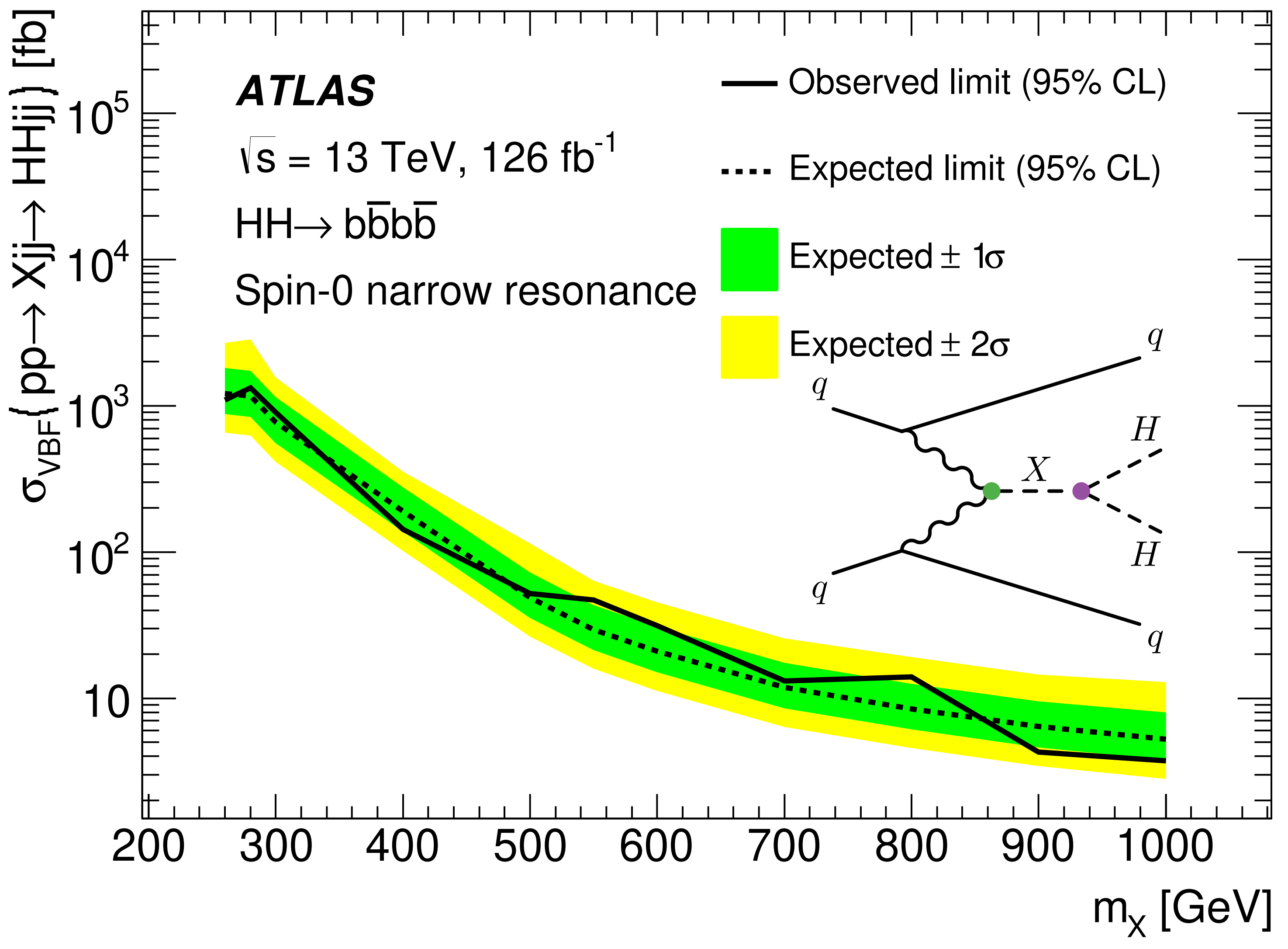

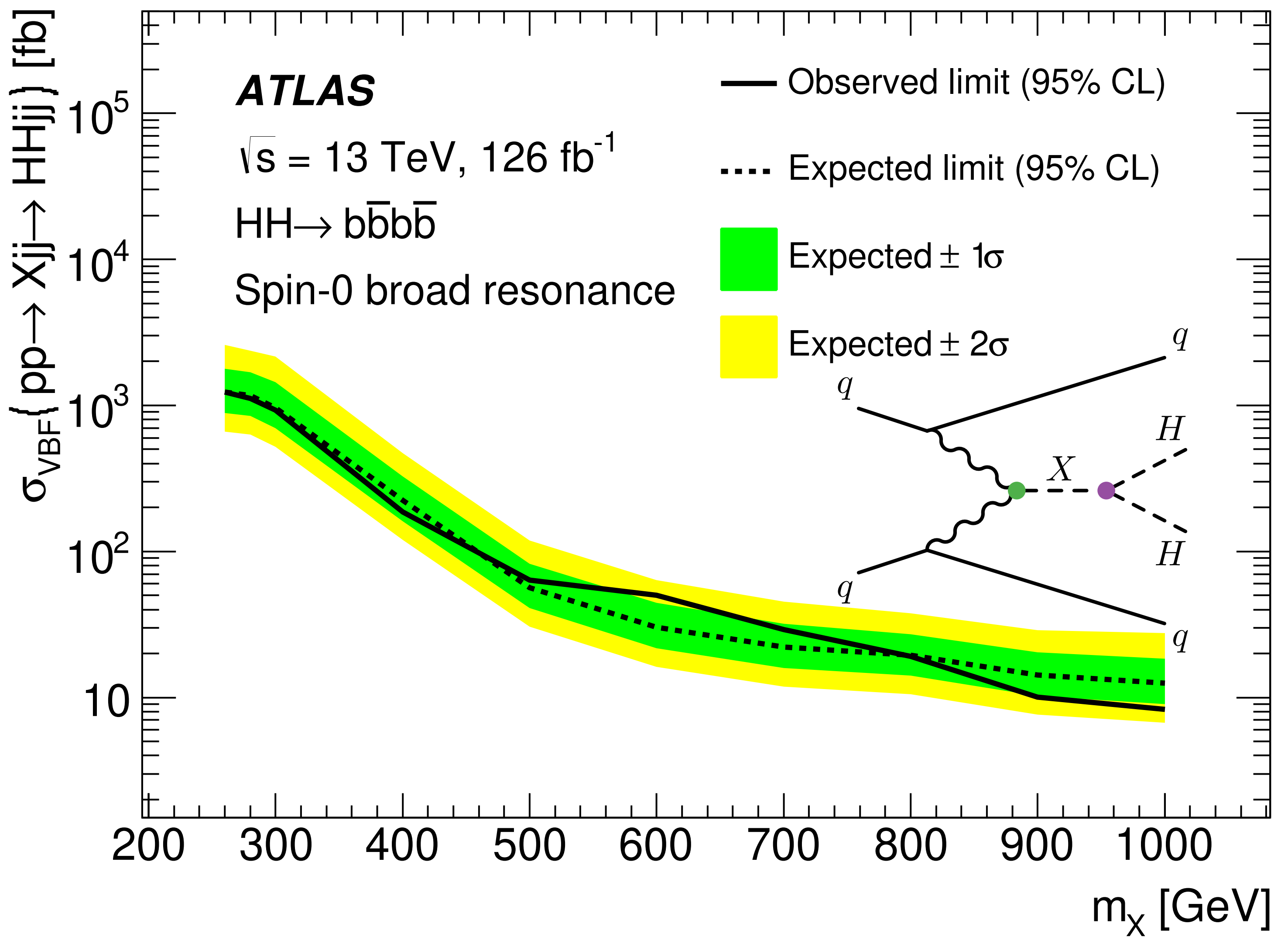

	Observed	-2σ	-1σ	Expected	$+1\sigma$	$+2\sigma$
σ_{VBF} [fb]	1450	500	660	920	1280	1720
$\sigma_{\mathrm{VBF}}/\sigma_{\mathrm{VBF}}^{\mathrm{SM}}$	840	290	390	540	750	1000

$\kappa_{2V} < -0.43$ and $\kappa_{2V} > 2.56$ excluded at 95% CL

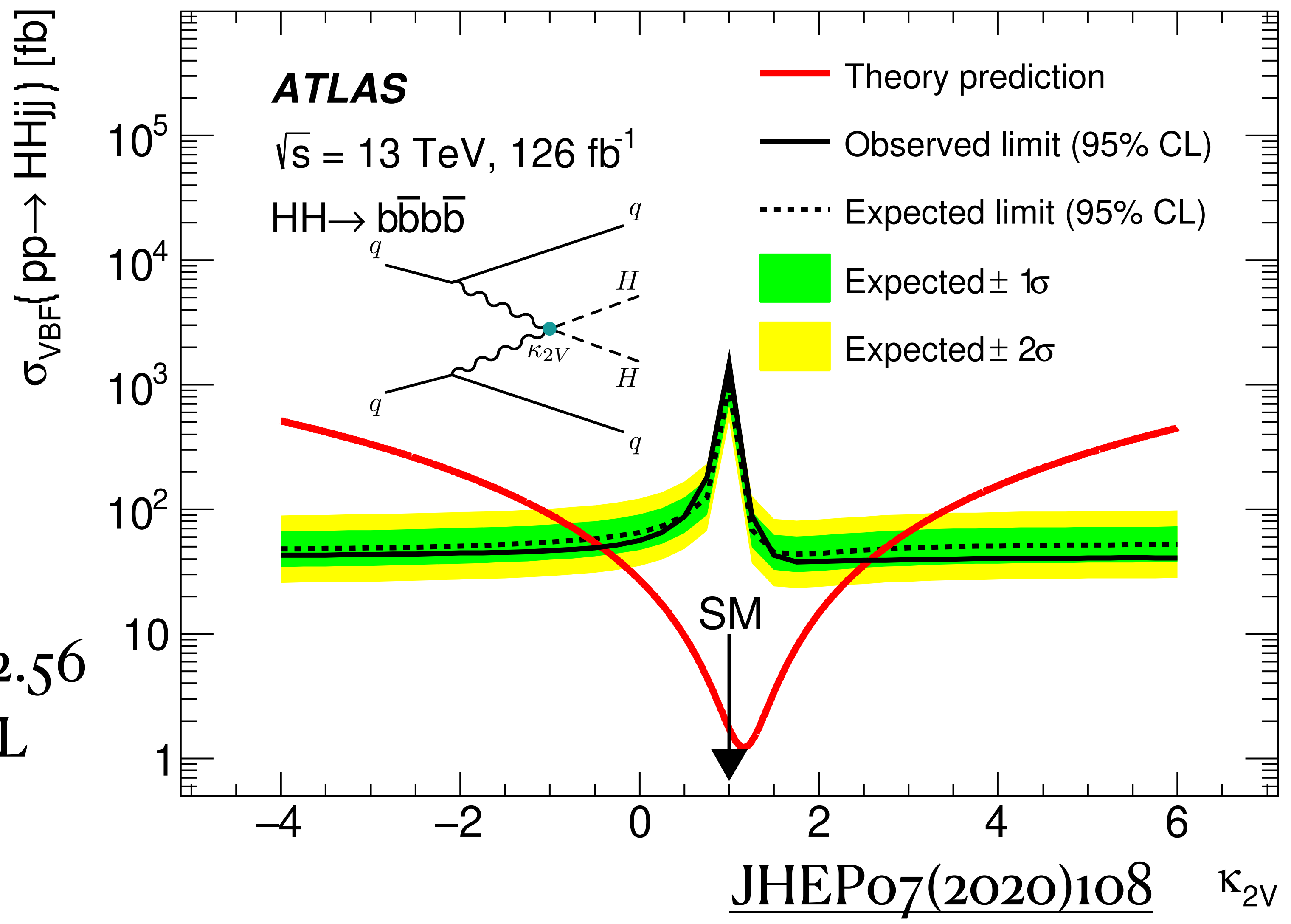

JHEP07(2020)108

$HH \to b\bar{b}\ell\nu\ell\nu$

- HH analysis with one Higgs decaying via $H \to b\bar{b}$ and the other via $H \to WW^*/ZZ^*/\tau\tau$
  - $\geq$ 2 b-tagged jets and exactly two leptons (electrons or muons) with opposite electric charge in the final state
- Analysis selection using a neural network classifier (input variables in backup)

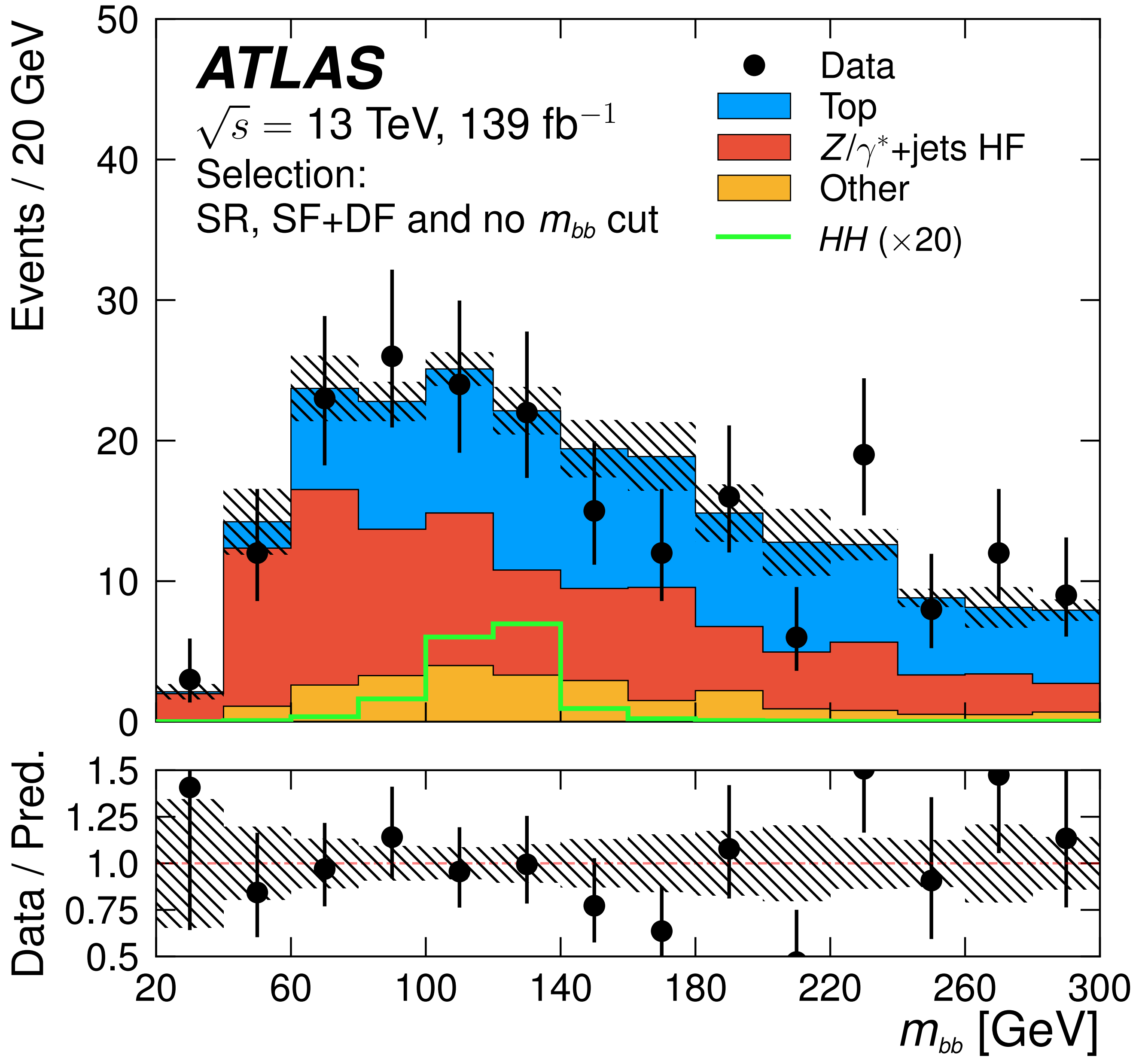

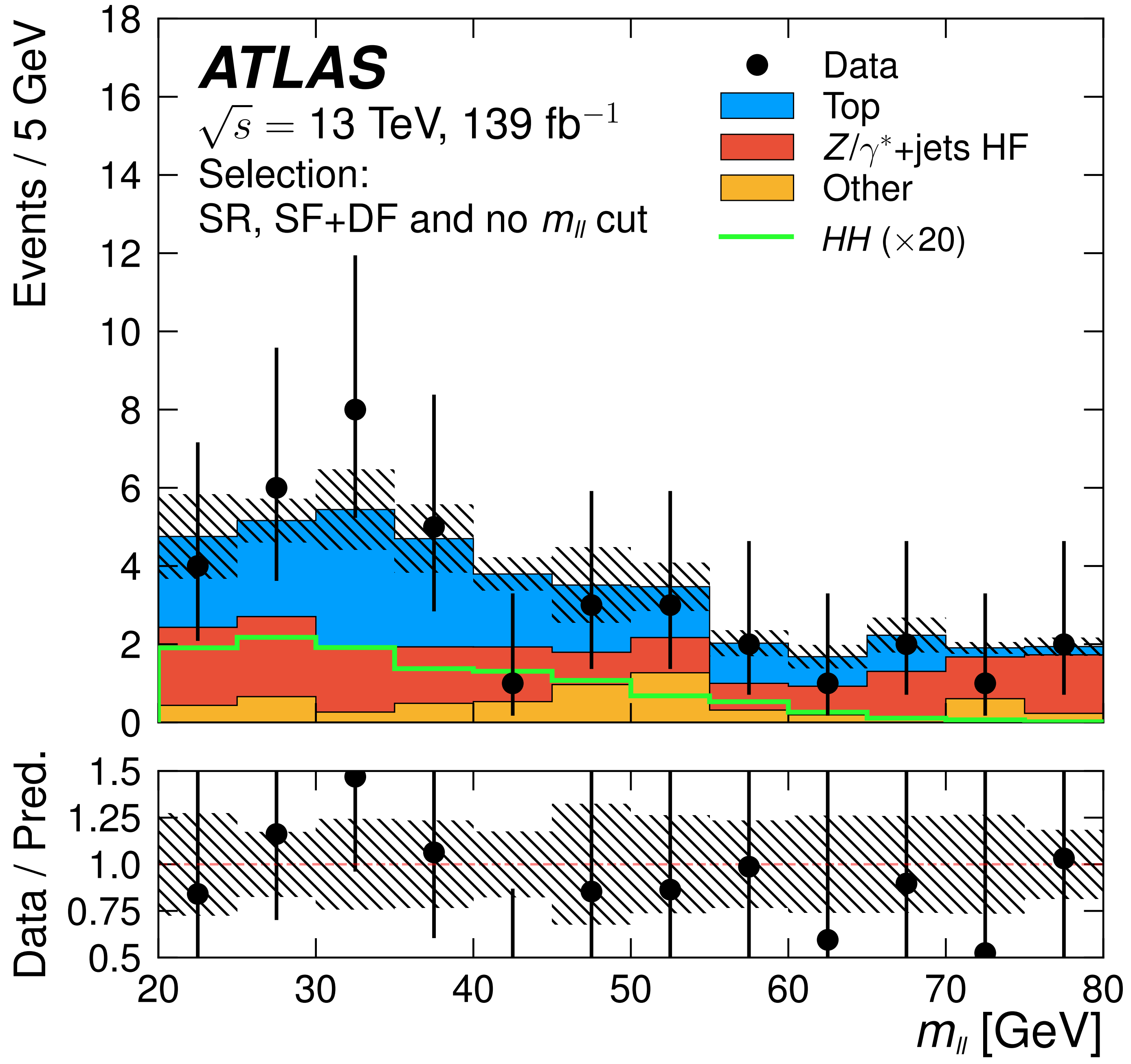

Phys. Lett. B 801 (2020) 135145

$HH \to b\bar{b}\ell\nu\ell\nu$

- Limits extracted from counting experiment fit in regions defined by
    - Neural network score (d_{HH})
    - Lepton flavor: same flavor (SF: ee, $\mu\mu$) or different flavor (DF: $e\mu$)
    - Dilepton and $b\bar{b}$ invariant mass ($m_{\ell\ell}$, m_{bb})
- No excess of data over background observed. Limits are set on the cross-section for non-resonant HH production

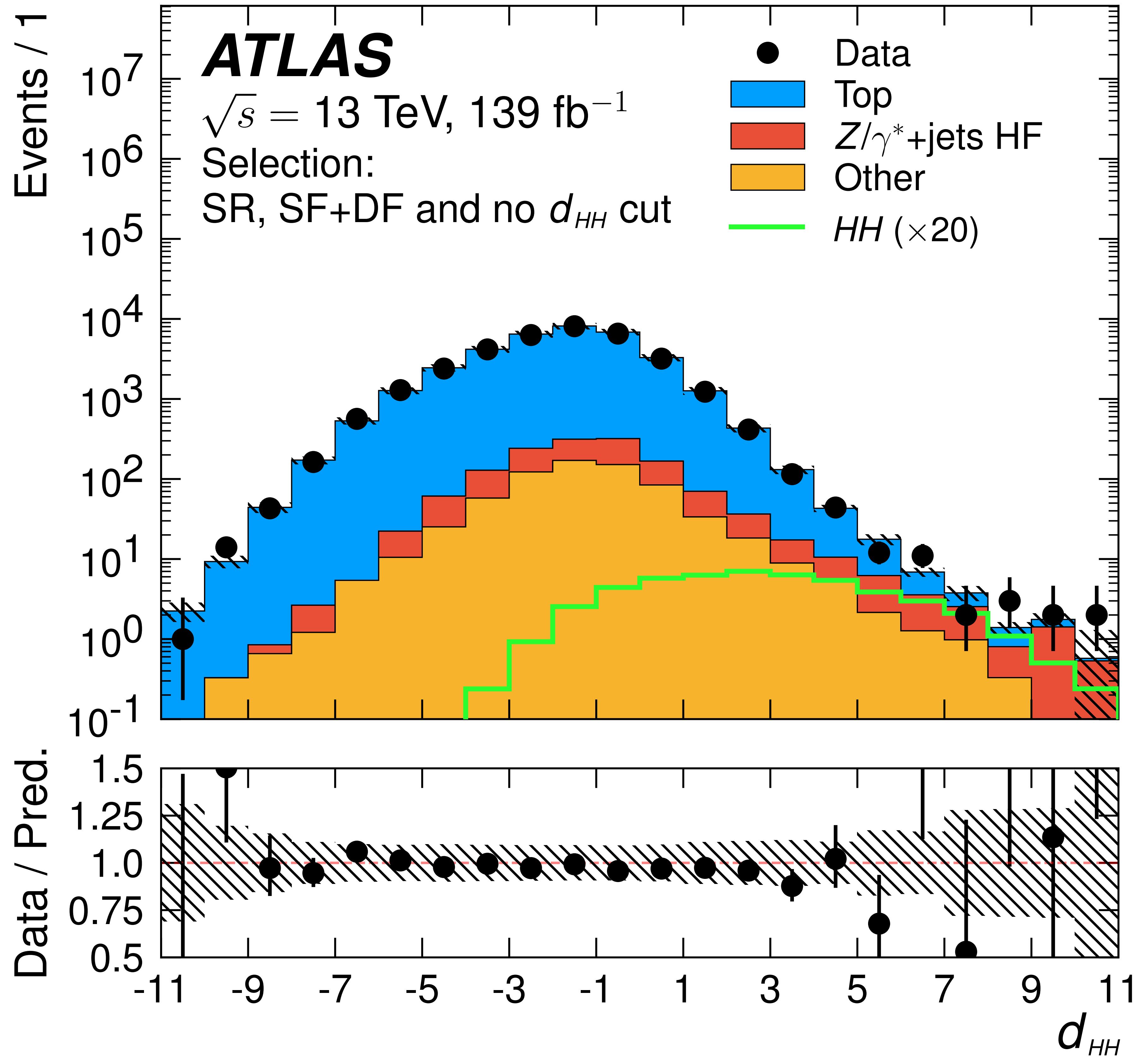

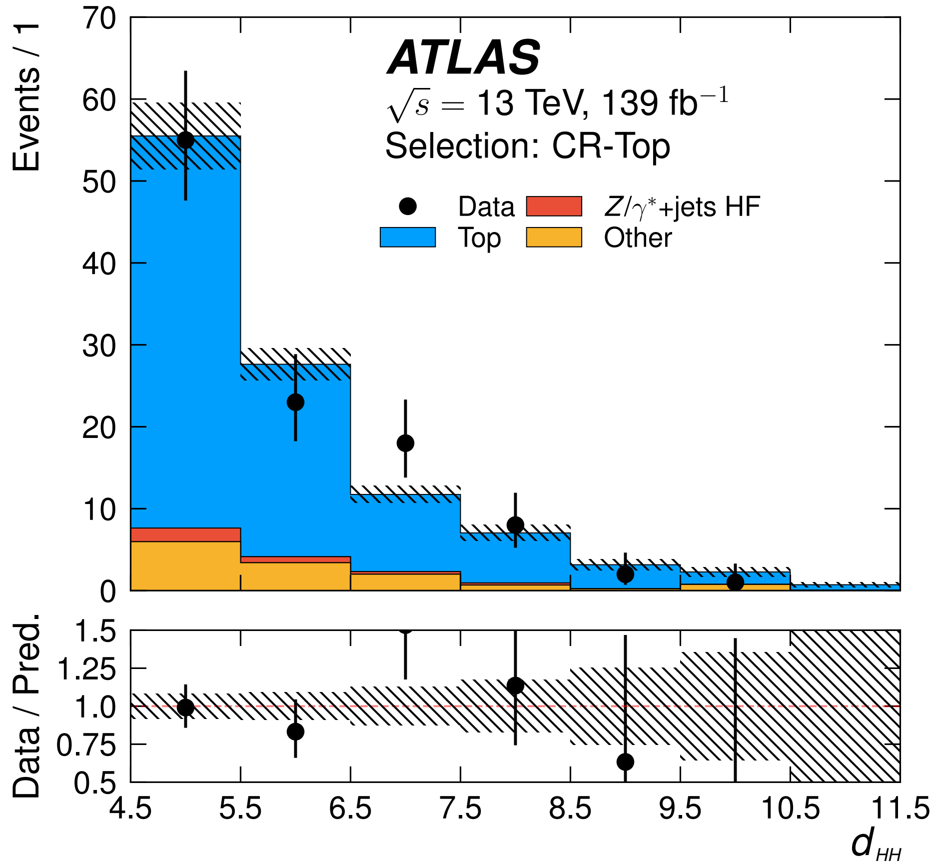

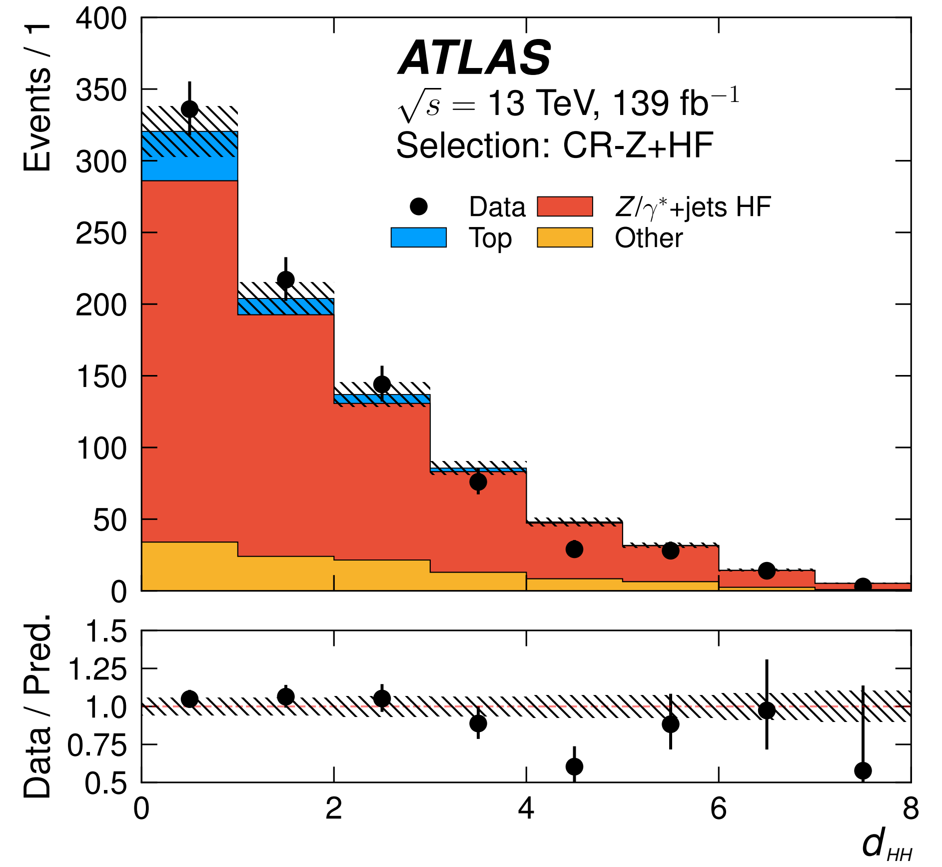

	-2σ	-1σ	**Expected**	$+1\sigma$	$+2\sigma$	**Observed**
$\sigma\,(gg \to HH)$ [pb]	0.5	0.6	0.9	1.3	1.9	1.2
$\sigma\,(gg \to HH)/\sigma^{\mathrm{SM}}\,(gg \to HH)$	14	20	29	43	62	40

Phys. Lett. B 801 (2020) 135145

$HH \to b\bar{b}\gamma\gamma$

- Both a resonant and a non-resonant search performed
- BDTs used for signal/background discrimination (see backup for inputs)
- A “corrected” definition of $m_{b\bar{b}\gamma\gamma}$ (candidate HH invariant mass) is used here, which improves resolution (backup)

$$m^*_{b\bar{b}\gamma\gamma} \equiv m_{b\bar{b}\gamma\gamma} - m_{b\bar{b}} - m_{\gamma\gamma} + 250 \text{ GeV}$$

- Resonant search:
  - Signal extraction performed in a BDT window based on resonance mass
  - Final discriminant is invariant mass of $\gamma\gamma$

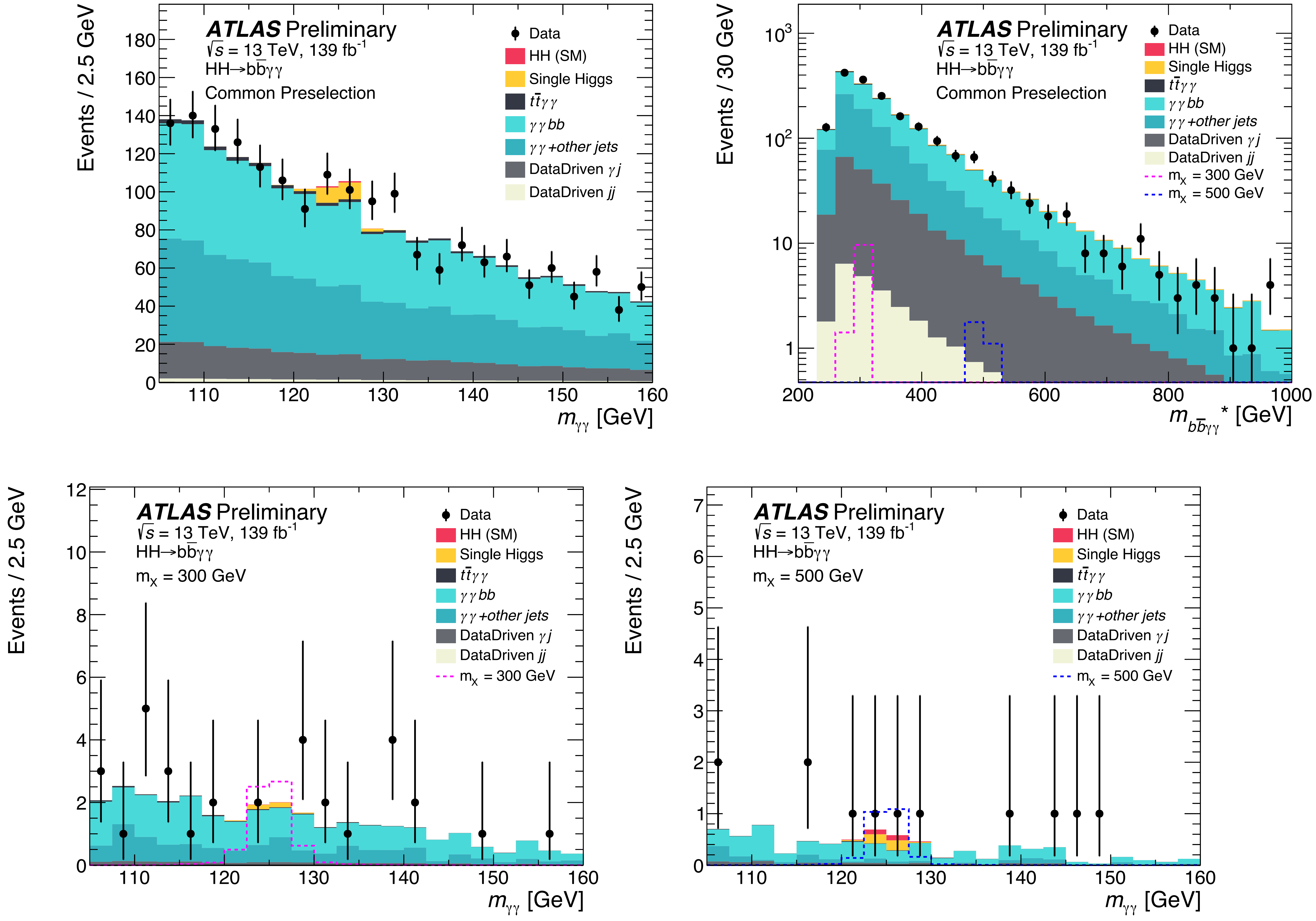

ATLAS-CONF-2021-016

$HH \to b\bar{b}\gamma\gamma$

- Non-resonant search:
  - Four categories considered based on BDT score and $m^*_{b\bar{b}\gamma\gamma}$:
    - High mass region: $m^*_{b\bar{b}\gamma\gamma} \geq 350$ GeV, targets the SM signal (κ_λ = 1)
    - Low mass region: $m^*_{b\bar{b}\gamma\gamma} < 350$ GeV, used to retain sensitivity for BSM signals (e.g. κ_λ = 10)
    - In each mass category, two regions are created with a loose/tight BDT cut
  - Fit performed simultaneously in all four categories
  - ggF and VBF production mode included for non-resonant

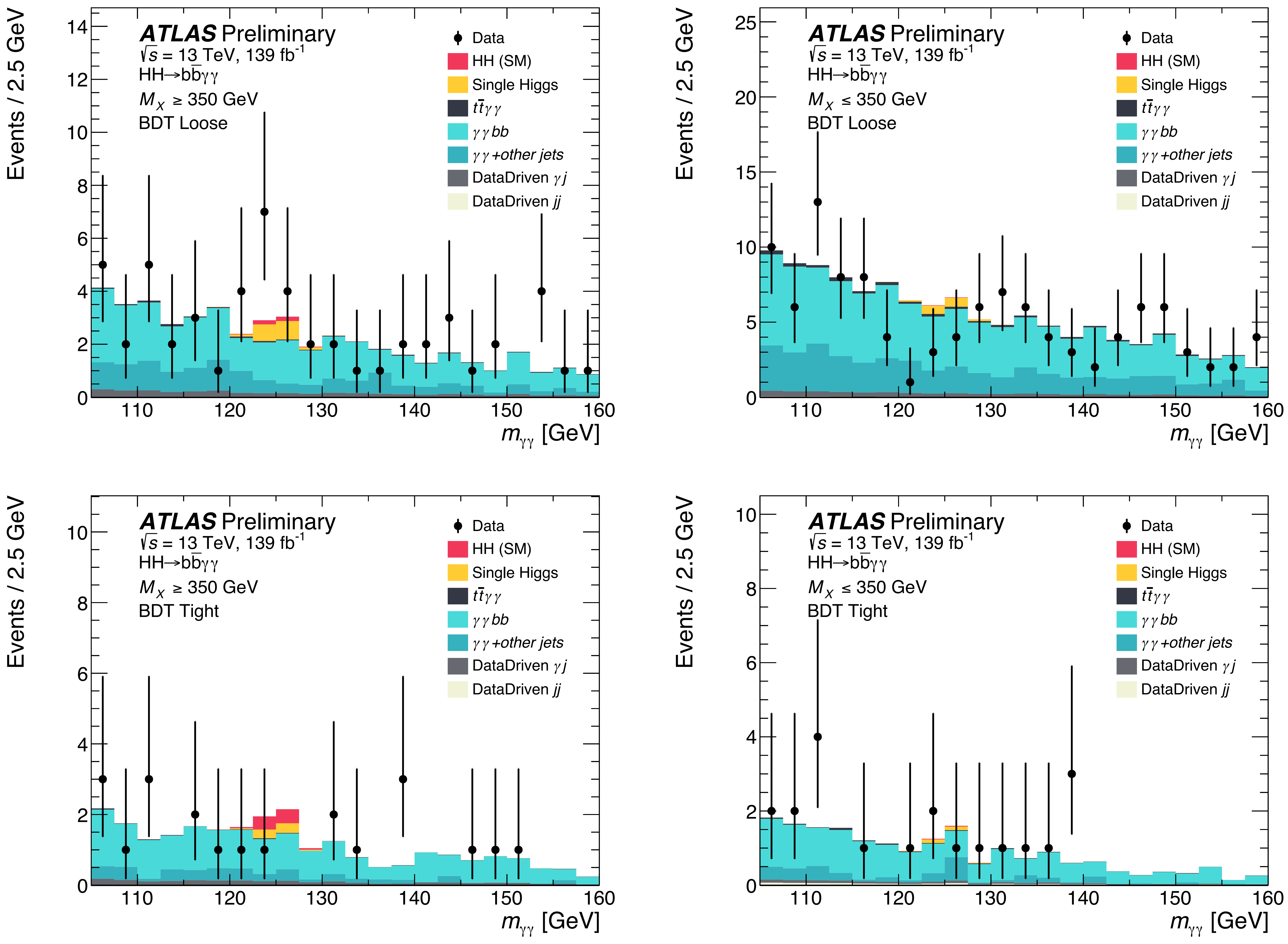

ATLAS-CONF-2021-016

$HH \to bb\gamma\gamma$

- No significant excesses found
- Limits set on narrow width scalar resonances from 251 GeV to 1000 GeV
- κ_λ constraints:
  - Observed: $-1.5 < \kappa_\lambda < 6.7$
  - Expected: $-2.4 < \kappa_\lambda < 7.7$

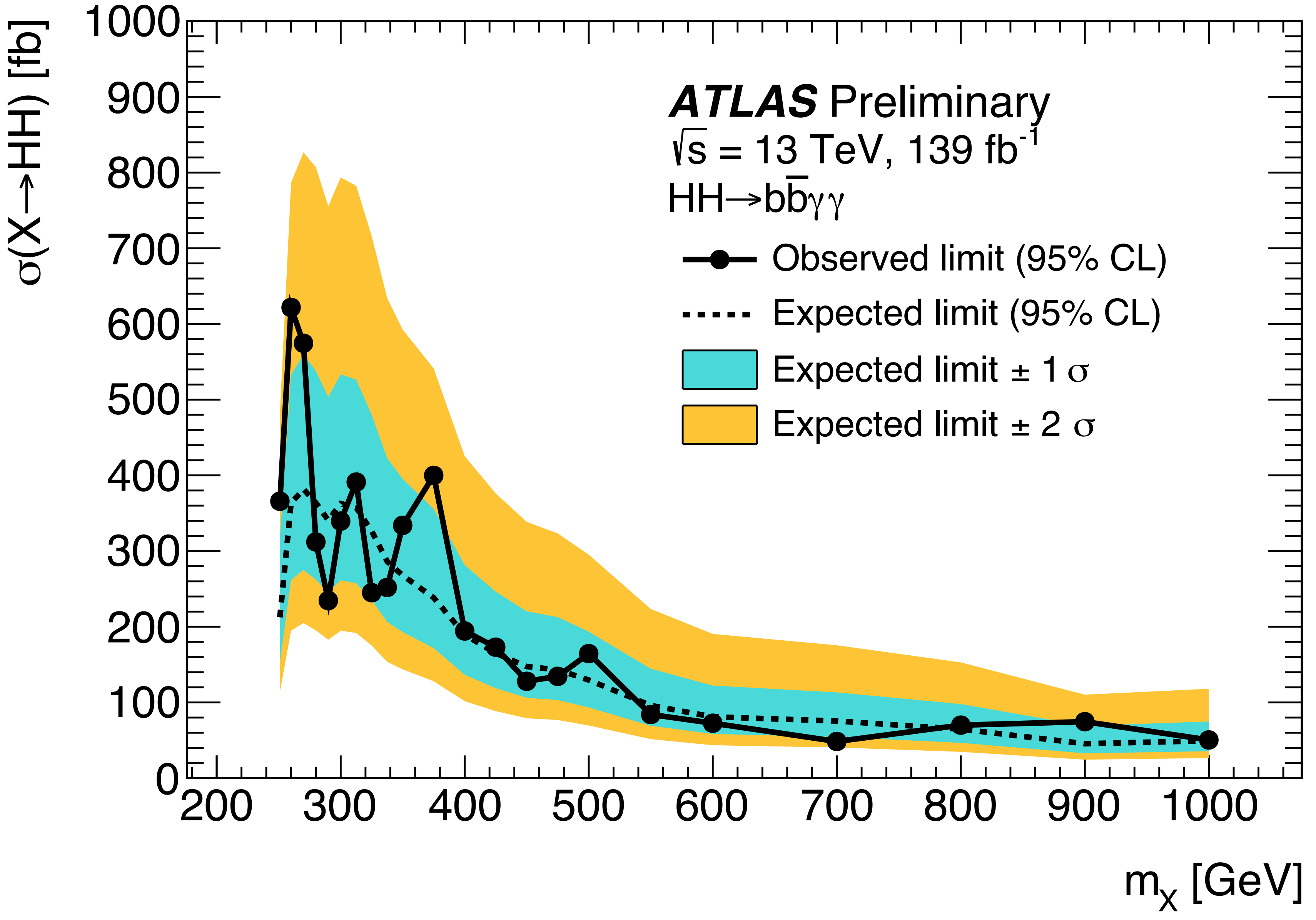

Observed (expected) limit:
4.1 (5.5) x SM cross section

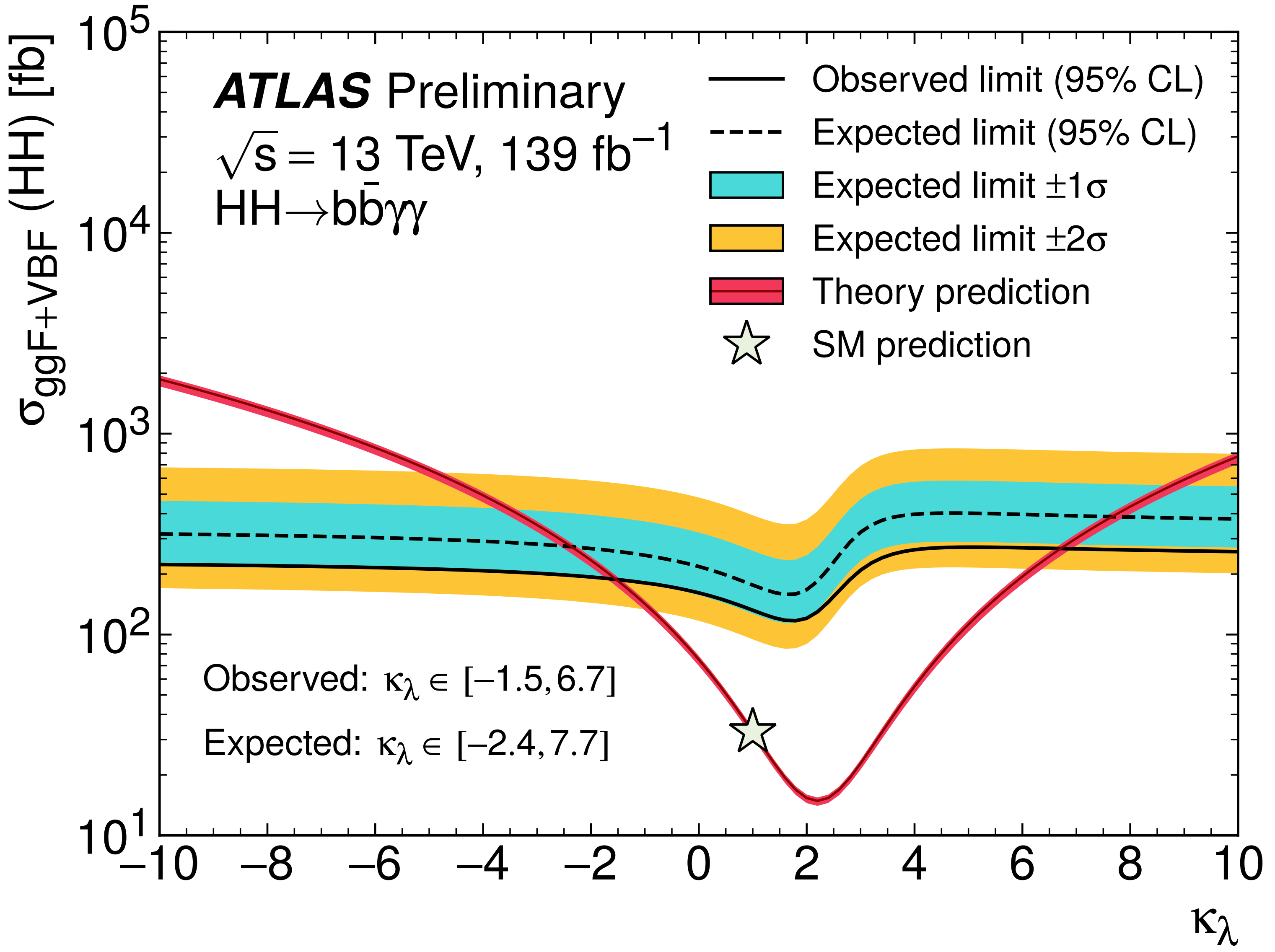

ATLAS-CONF-2021-016

HL-LHC Prospects

- Prospects study for non-resonant HH production at the HL-LHC using $b\bar{b}b\bar{b}$, $b\bar{b}\tau^+\tau^-$, and $b\bar{b}\gamma\gamma$ final states
  - 3000 fb^{-1} assumed = ~20 x full Run 2 dataset
  - $b\bar{b}b\bar{b}$, $b\bar{b}\tau^+\tau^-$ projections of early Run 2 analyses, $b\bar{b}\gamma\gamma$ simulation-based
- Expected signal strength for SM:
  3.5σ (no systematic uncertainties)
  3.0σ (with systematic uncertainties)
- Much effort ongoing in the collaboration – can we push this further?

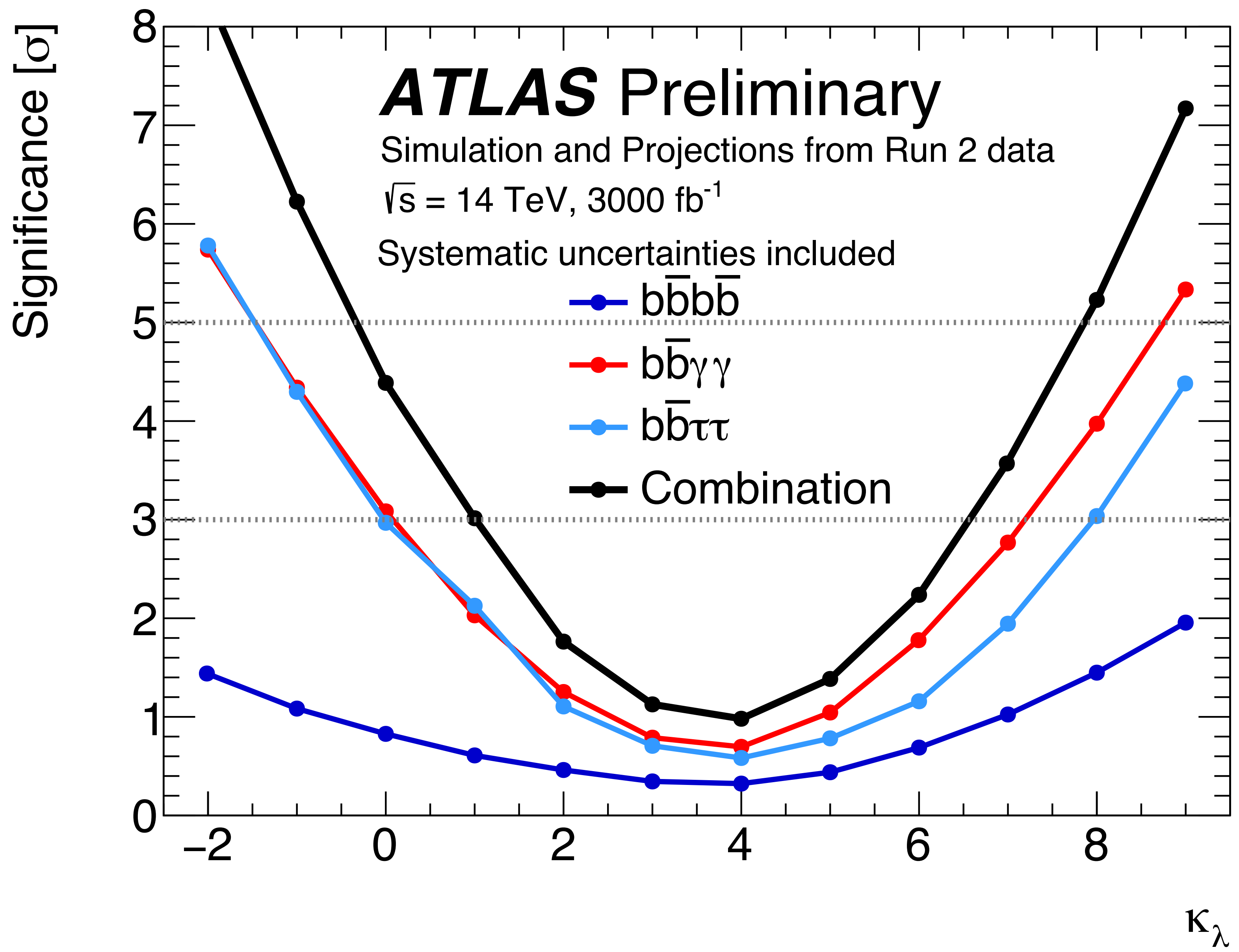

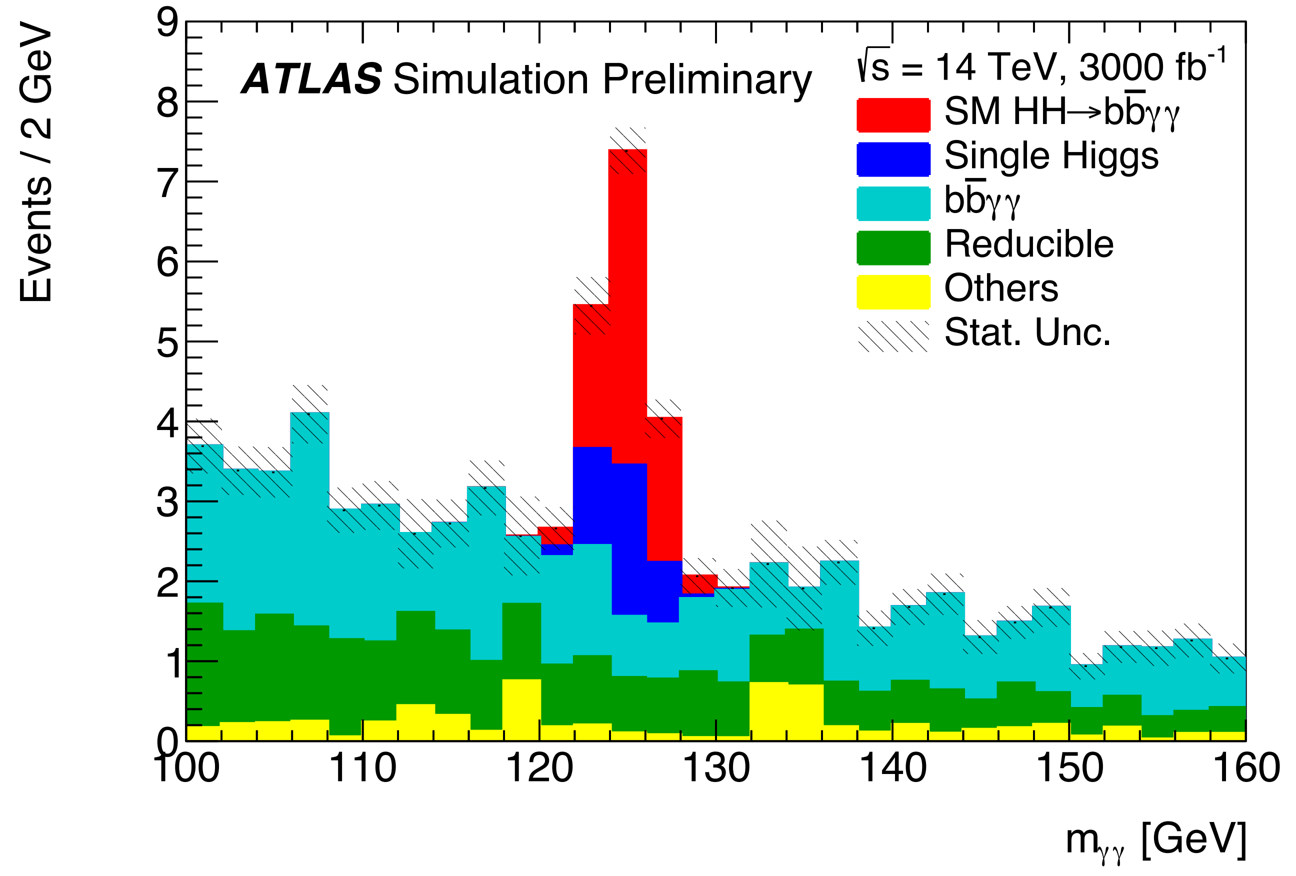

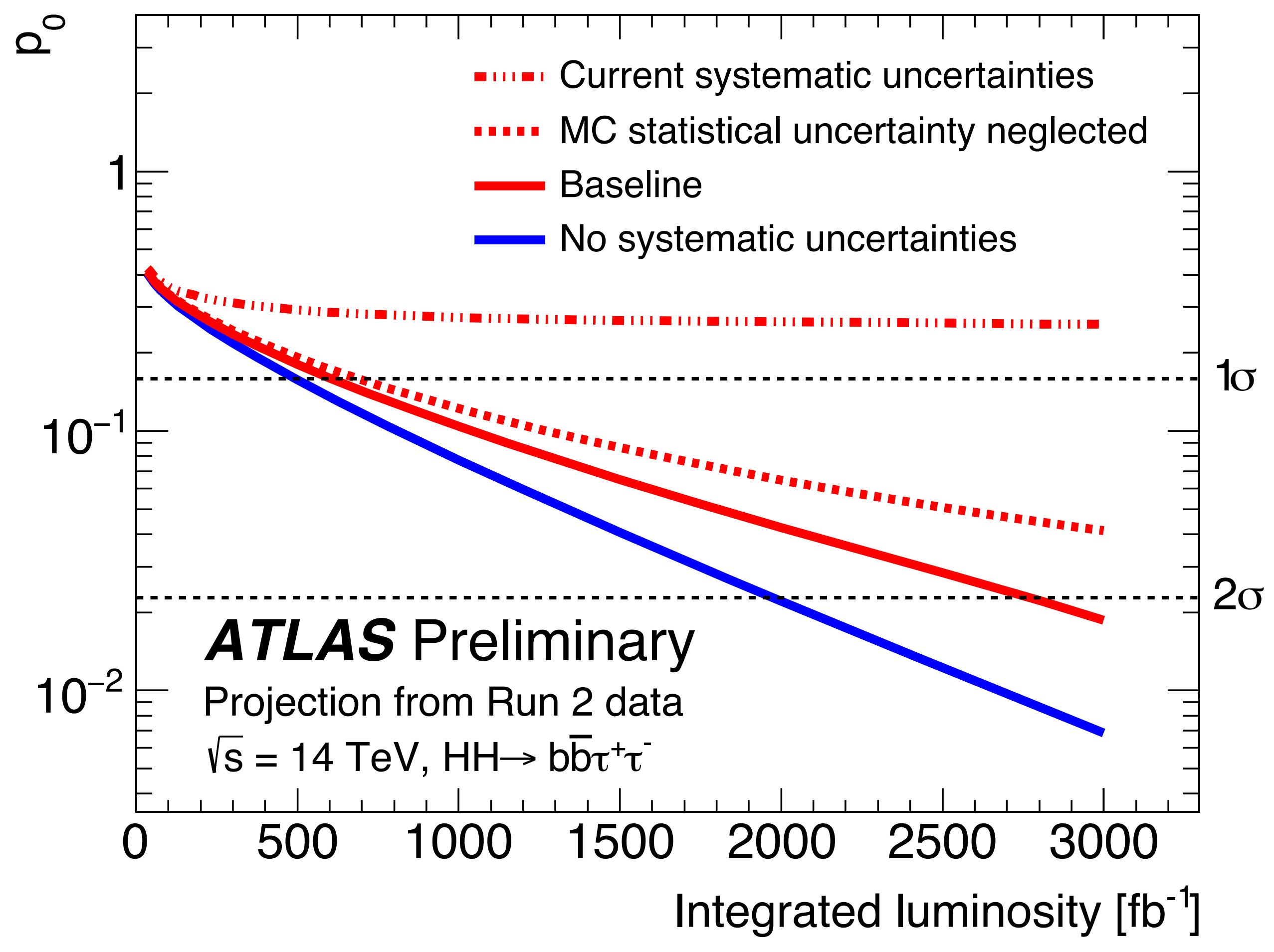

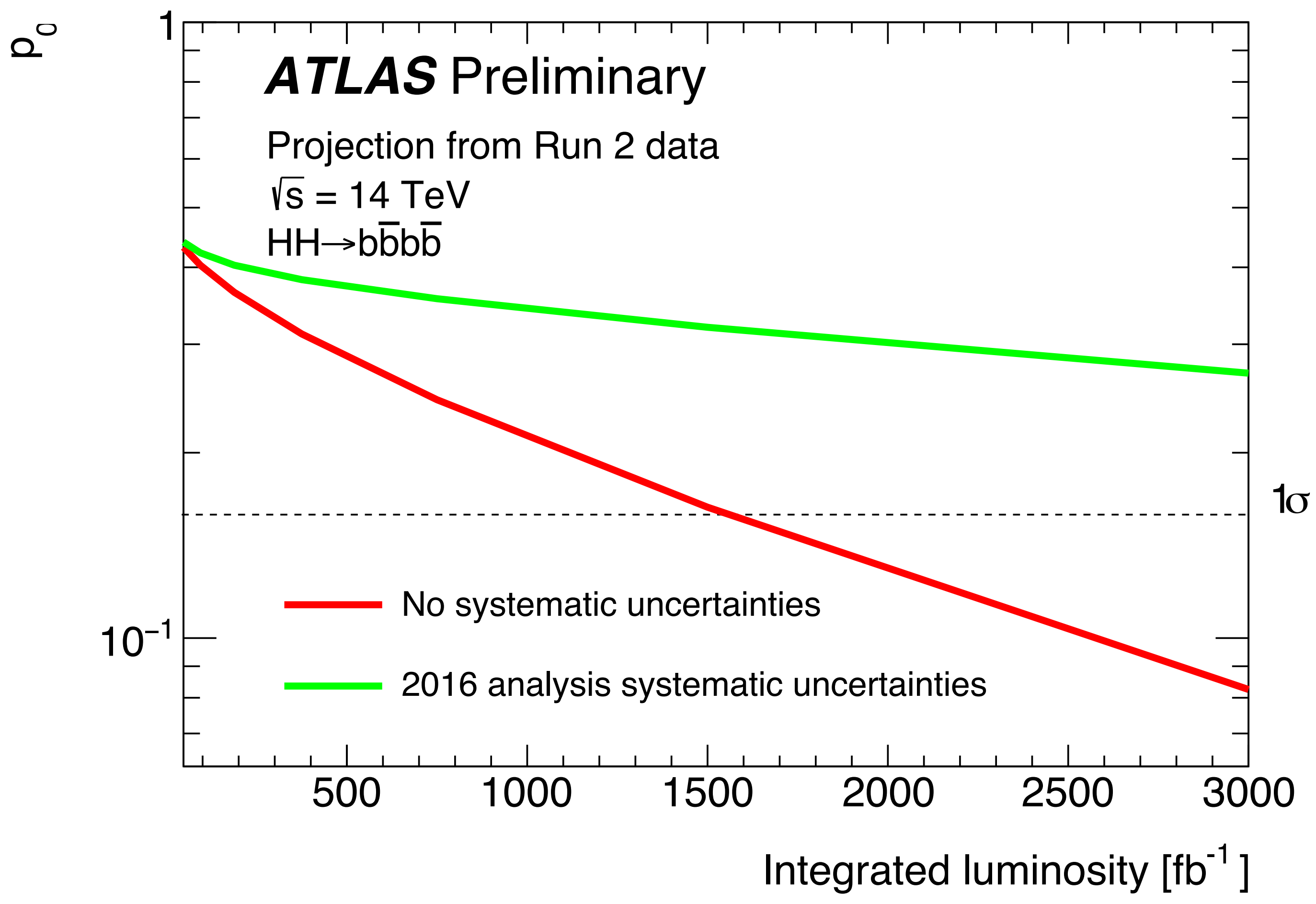

ATL-PHYS-PUB-2018-053

Conclusions

- Full LHC Run 2 ATLAS searches for HH have been presented for a variety of channels
- No significant excesses of data over background seen
- Limits set on a variety of scalar resonances, as well as variations of the trilinear Higgs coupling **(HHH)**, the coupling between a Higgs boson pair and two vector bosons **(VVHH)**, and the SM HH production cross-section
- Prospects for the HL-LHC based on early Run 2 analyses have been shown – the future is bright!
- The collaboration is HHard at work – stay tuned for more!

Backup

Boosted $HH \rightarrow b\bar{b}\tau^+\tau^-$

- Variables used in the di-τ tagger BDT
  - Distinguish di-τ object from quark/gluon initiated jets

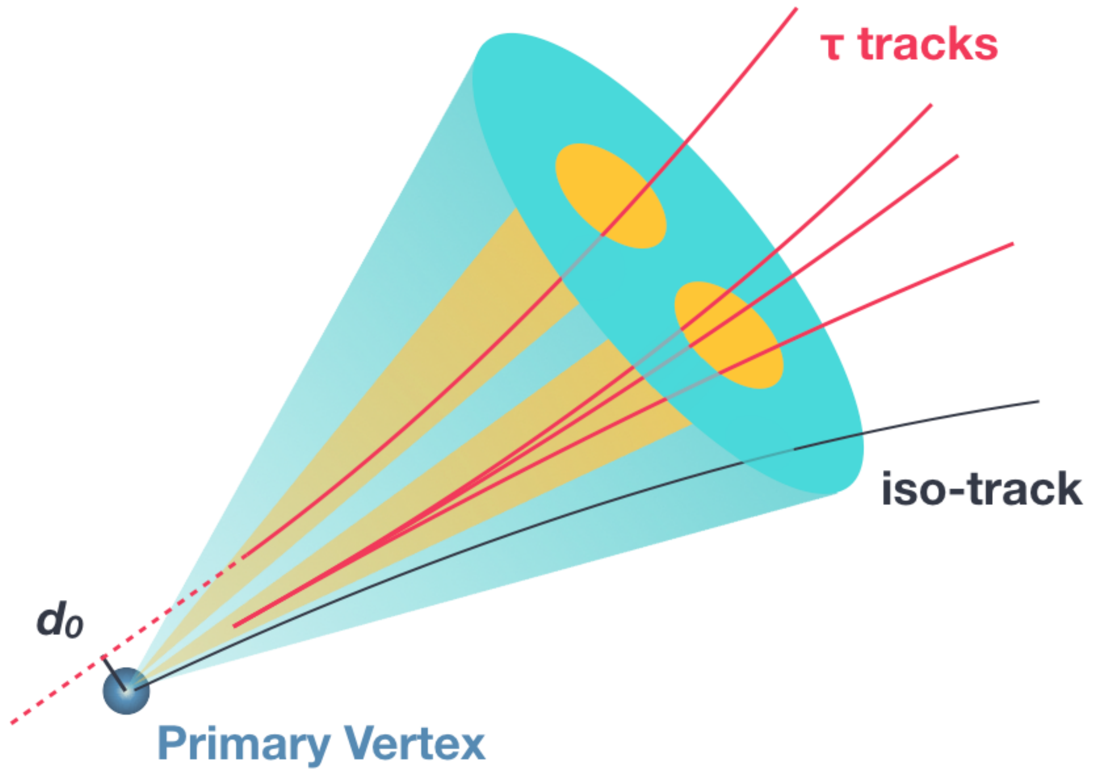

Variable	Definition
$E^{\mathrm{sj}_1}_{\Delta R<0.1}/E^{\mathrm{sj}_1}_{\Delta R<0.2}$ and $E^{\mathrm{sj}_2}_{\Delta R<0.1}/E^{\mathrm{sj}_2}_{\Delta R<0.2}$	Ratios of the energy deposited in the core to that in the full cone, for the sub-jets sj_1 and sj_2, respectively
$p^{\mathrm{sj}_2}_{\mathrm{T}}/p^{\mathrm{LRJ}}_{\mathrm{T}}$ and $(p^{\mathrm{sj}_1}_{\mathrm{T}}+p^{\mathrm{sj}_2}_{\mathrm{T}})/p^{\mathrm{LRJ}}_{\mathrm{T}}$	Ratio of the p_{T} of sj_2 to the di-τ seeding large-radius jet p_{T} and ratio of the scalar p_{T} sum of the two leading sub-jets to the di-τ seeding large-radius jet p_{T}, respectively
$\log(\sum p^{\text{iso-tracks}}_{\mathrm{T}}/p^{\mathrm{LRJ}}_{\mathrm{T}})$	Logarithm of the ratio of the scalar p_{T} sum of the iso-tracks to the di-τ seeding large-radius jet p_{T}
$\Delta R_{\max}(\text{track}, \mathrm{sj}_1)$ and $\Delta R_{\max}(\text{track}, \mathrm{sj}_2)$	Largest separation of a track from its associated sub-jet axis, for the sub-jets sj_1 and sj_2, respectively
$\sum[p^{\text{track}}_{\mathrm{T}}\Delta R(\text{track}, \mathrm{sj}_2)]/\sum p^{\text{track}}_{\mathrm{T}}$	p_{T}-weighted ΔR of the tracks matched to sj_2 with respect to its axis
$\sum[p^{\text{iso-track}}_{\mathrm{T}}\Delta R(\text{iso-track}, \mathrm{sj})]/\sum p^{\text{iso-track}}_{\mathrm{T}}$	p_{T}-weighted sum of ΔR between iso-tracks and the nearest sub-jet axis
$\log(m^{\text{tracks}, \mathrm{sj}_1}_{\Delta R<0.1})$ and $\log(m^{\text{tracks}, \mathrm{sj}_2}_{\Delta R<0.1})$	Logarithms of the invariant mass of the tracks in the core of sj_1 and sj_2, respectively
$\log(m^{\text{tracks}, \mathrm{sj}_1}_{\Delta R<0.2})$ and $\log(m^{\text{tracks}, \mathrm{sj}_2}_{\Delta R<0.2})$	Logarithms of the invariant mass of the tracks with $\Delta R < 0.2$ from the axis of sj_1 and sj_2, respectively
$\log(\lvert d^{\mathrm{sj}_1}_{0,\text{lead-track}}\rvert)$ and $\log(\lvert d^{\mathrm{sj}_2}_{0,\text{lead-track}}\rvert)$	Logarithms of the closest distance in the transverse plane between the primary vertex and the leading track of sj_1 and sj_2, respectively
$n^{\mathrm{sj}_1}_{\text{tracks}}$ and $n^{\text{sub-jets}}_{\text{tracks}}$	Number of tracks matched to sj_1 and to all sub-jets, respectively

JHEP11(2020)163

$HH \to b\bar{b}\ell\nu\ell\nu$

- Variables used for the signal vs. background DNN classifier

(p_T, η, ϕ)	p_T, η, and ϕ of the leptons, leading two signal jets, and leading two b-tagged jets
Dilepton flavour	Whether the event is composed of two electrons, two muons, or one of each
$\Delta R_{\ell\ell}$, $\lvert\Delta\phi_{\ell\ell}\rvert$	ΔR and magnitude of the $\Delta\phi$ between the two leptons
$m_{\ell\ell}$, $p_T^{\ell\ell}$	Invariant mass and the transverse momentum of the dilepton system
$E_{\mathrm{T}}^{\mathrm{miss}}$, $E_{\mathrm{T}}^{\mathrm{miss}}$-$\phi$	Magnitude of the missing transverse momentum vector and its ϕ component
$\lvert\Delta\phi(\mathbf{p}_{\mathrm{T}}^{\mathrm{miss}}, \mathbf{p}_{\mathrm{T}}^{\ell\ell})\rvert$	Magnitude of the $\Delta\phi$ between the $\mathbf{p}_{\mathrm{T}}^{\mathrm{miss}}$ and the transverse momentum of the dilepton system
$\lvert\mathbf{p}_{\mathrm{T}}^{\mathrm{miss}} + \mathbf{p}_{\mathrm{T}}^{\ell\ell}\rvert$	Magnitude of the vector sum of the $\mathbf{p}_{\mathrm{T}}^{\mathrm{miss}}$ and the transverse momentum of the dilepton system
Jet multiplicities	Numbers of b-tagged and non-b-tagged jets
$\lvert\Delta\phi_{bb}\rvert$	Magnitude of the $\Delta\phi$ between the leading two b-tagged jets
m_{T2}^{bb}	m_{T2} [119] using the leading two b-tagged jets as the visible inputs and $\mathbf{p}_{\mathrm{T}}^{\mathrm{miss}}$ as invisible input
H_{T2}	Scalar sum of the magnitudes of the momenta of the $H \to \ell\nu\ell\nu$ and $H \to bb$ systems, $H_{\mathrm{T2}} = \lvert\mathbf{p}_{\mathrm{T}}^{\mathrm{miss}} + \mathbf{p}_{\mathrm{T}}^{\ell,0} + \mathbf{p}_{\mathrm{T}}^{\ell,1}\rvert + \lvert\mathbf{p}_{\mathrm{T}}^{b,0} + \mathbf{p}_{\mathrm{T}}^{b,1}\rvert$
$H_{\mathrm{T2}}^{\mathrm{R}}$	Ratio of H_{T2} and scalar sum of the transverse momenta of the H decay products, $H_{\mathrm{T2}}^{\mathrm{R}} = H_{\mathrm{T2}}/(E_{\mathrm{T}}^{\mathrm{miss}} + \lvert\mathbf{p}_{\mathrm{T}}^{\ell,0}\rvert + \lvert\mathbf{p}_{\mathrm{T}}^{\ell,1}\rvert + \lvert\mathbf{p}_{\mathrm{T}}^{b,0}\rvert + \lvert\mathbf{p}_{\mathrm{T}}^{b,1}\rvert)$, where $\mathbf{p}_{\mathrm{T}}^{\ell(b),0\{1\}}$ are the transverse momenta of the leading {subleading} lepton (b-tagged jet)

Phys. Lett. B 801 (2020) 135145

$HH \to b\bar{b}\ell\nu\ell\nu$

- Region definitions based on dilepton flavor, $m_{\ell\ell}$, $m_{b\bar{b}}$, and DNN score

Region Definitions						
Observable	**CR-Top**	**VR-1**	**CR-Z+HF**	**VR-2**	**SR-SF**	**SR-DF**
Dilepton Flavour	DF	SF	DF or SF	SF	SF	DF
$m_{\ell\ell}$ [GeV]	(20, 60)	(20, 60)	(81.2, 101.2)	(71.2, 81.2) or (101.2, 115)	(20, 60)	(20, 60)
m_{bb} [GeV]	$\notin$ (100, 140)	> 140	(100, 140)	(100, 140)	(110, 140)	(110, 140)
d_{HH}	> 4.5	> 4.5	> 0	> 0	> 5.45	> 5.55
Event Yields						
Data	108	171	852	157	16	9
Total Bkg.	108 ± 10	162 ± 10	852 ± 29	147 ± 11	14.9 ± 2.1	4.9 ± 1.2
Top	92 ± 11	77 ± 10	55 ± 7	71 ± 10	4.8 ± 1.4	3.8 ± 1.1
Z/γ^*+ HF	3.2 ± 0.5	70 ± 4	686 ± 33	60 ± 4	7.8 ± 1.4	0.21 ± 0.05
Other	13.1 ± 3.4	14.2 ± 1.9	110 ± 13	15.8 ± 1.2	2.3 ± 0.5	0.9 ± 0.4
HH (×20)	2.70 ± 0.25	1.03 ± 0.22	1.97 ± 0.11	1.22 ± 0.05	5.0 ± 0.6	4.8 ± 0.8
Post-fit Normalisation						
$\mu_{\text{Top}} = 0.79 \pm 0.10$			$\mu_{Z/\gamma^*+\text{HF}} = 1.36 \pm 0.07$			

Phys. Lett. B 801 (2020) 135145

VBF $HH \to b\bar{b}b\bar{b}$

- Table illustrating cuts used for VBF 4b analysis
- Note that the selection builds off of that used for the early Run 2 gluon-gluon fusion result

	Selections	
VBF topology	At least two jets with $p_T > 30$, $\lvert\eta\rvert > 2.0$	Two highest-p_T jets with opposite sign η
		$\left\lvert\Delta\eta_{jj}^{VBF}\right\rvert > 5.0$ and $m_{jj}^{VBF} > 1000$
Signal topology	Exactly 4 b-tagged jets with $p_T > 40$, $\lvert\eta\rvert < 2.0$	
	If $m_{4b} < 1250$	$\frac{360}{m_{4b}} - 0.5 < \Delta R_{bb}^{lead} < \frac{653}{m_{4b}} + 0.475$
		$\frac{235}{m_{4b}} < \Delta R_{bb}^{subl} < \frac{875}{m_{4b}} + 0.35$
	If $m_{4b} \geq 1250$	$\Delta R_{bb}^{lead} < 1$
		$\Delta R_{bb}^{subl} < 1$
	Pairs with minimum $D_{HH} = \sqrt{(m_{2b}^{lead})^2 + (m_{2b}^{subl})^2}\left\lvert\sin\left(\tan^{-1}\left(\frac{m_{2b}^{subl}}{m_{2b}^{lead}}\right) - \tan^{-1}\left(\frac{116.5}{123.7}\right)\right)\right\rvert$	
Background rejection	Multijet	$\lvert\Delta\eta_{HH}\rvert < 1.5$
		$\lvert\Sigma_i \vec{p}_{T_i}\rvert < 60$, where i = b-jets and VBF-jets
		$p_{T,H}^{lead} > 0.5 m_{4b} - 103$
		$p_{T,H}^{subl} > 0.33 m_{4b} - 73$
	$t\bar{t}$	Veto if $X_{Wt} = \sqrt{\left(\frac{m_W - 80.4}{0.1 m_W}\right)^2 + \left(\frac{m_t - 172.5}{0.1 m_t}\right)^2} \leq 1.5$
Region definition	Signal region (SR)	$X_{HH} = \sqrt{\left(\frac{m_{2b}^{lead} - 123.7}{11.6}\right)^2 + \left(\frac{m_{2b}^{subl} - 116.5}{18.1}\right)^2} < 1.6$
	Validation region (veto SR)	$\sqrt{\left(m_{2b}^{lead} - 123.7\right)^2 + \left(m_{2b}^{subl} - 116.5\right)^2} < 30$
	Sideband region (veto SR, VR)	$\sqrt{\left(m_{2b}^{lead} - 123.7\right)^2 + \left(m_{2b}^{subl} - 116.5\right)^2} < 45$

JHEP07(2020)108

$HH \to b\bar{b}\gamma\gamma$

- Variables used in the BDT for the resonant analysis

Variable	Definition
Photon-related kinematic variables	
$p_{\mathrm{T}}^{\gamma\gamma}$, $y^{\gamma\gamma}$	Transverse momentum and rapidity of the di-photon system
$\Delta\phi_{\gamma\gamma}$ and $\Delta R_{\gamma\gamma}$	Azimuthal angular distance and ΔR between the two photons
Jet-related kinematic variables	
$m_{b\bar{b}}$, $p_{\mathrm{T}}^{b\bar{b}}$ and $y_{b\bar{b}}$	Invariant mass, transverse momentum and rapidity of the b-tagged jets system
$\Delta\phi_{b\bar{b}}$ and $\Delta R_{b\bar{b}}$	Azimuthal angular distance and ΔR between the two b-tagged jets
N_{jets} and $N_{b-\mathrm{jets}}$	Number of jets and number of b-tagged jets
H_{T}	Scalar sum of the p_{T} of the jets in the event
Photons and jets-related kinematic variables	
$m_{b\bar{b}\gamma\gamma}$	Invariant mass built with the di-photon and b-tagged jets system
$\Delta y_{\gamma\gamma,b\bar{b}}$, $\Delta\phi_{\gamma\gamma,b\bar{b}}$ and $\Delta R_{\gamma\gamma,b\bar{b}}$	Distance in rapidity, azimuthal angle and ΔR between the di-photon and the b-tagged jets system

ATLAS-CONF-2021-016

$HH \to b\bar{b}\gamma\gamma$

- Variables used in the BDT for the non-resonant analysis

Variable	Definition
Photon-related kinematic variables	
$p_{\mathrm{T}}/m_{\gamma\gamma}$	Transverse momentum of the two photons scaled by their invariant mass $m_{\gamma\gamma}$
η and ϕ	Pseudo-rapidity and azimuthal angle of the leading and sub-leading photon
Jet-related kinematic variables	
b-tag status	Highest fixed b-tag working point that the jet passes
p_{T}, η and ϕ	Transverse momentum, pseudo-rapidity and azimuthal angle of the two jets with the highest b-tagging score
$p_{\mathrm{T}}^{b\bar{b}}$, $\eta_{b\bar{b}}$ and $\phi_{b\bar{b}}$	Transverse momentum, pseudo-rapidity and azimuthal angle of b-tagged jets system
$m_{b\bar{b}}$	Invariant mass built with the two jets with the highest b-tagging score
H_{T}	Scalar sum of the p_{T} of the jets in the event
Single topness	For the definition, see Eq. (1)
Missing transverse momentum-related variables	
$E_{\mathrm{T}}^{\mathrm{miss}}$ and ϕ^{miss}	Missing transverse momentum and its azimuthal angle

ATLAS-CONF-2021-016

$HH \to b\bar{b}\gamma\gamma$

- Plot showing resolution improvement from using $m^*_{b\bar{b}\gamma\gamma}$ vs. $m_{b\bar{b}\gamma\gamma}$, where

$$m^*_{b\bar{b}\gamma\gamma} \equiv m_{b\bar{b}\gamma\gamma} - m_{b\bar{b}} - m_{\gamma\gamma} + 250 \text{ GeV}$$

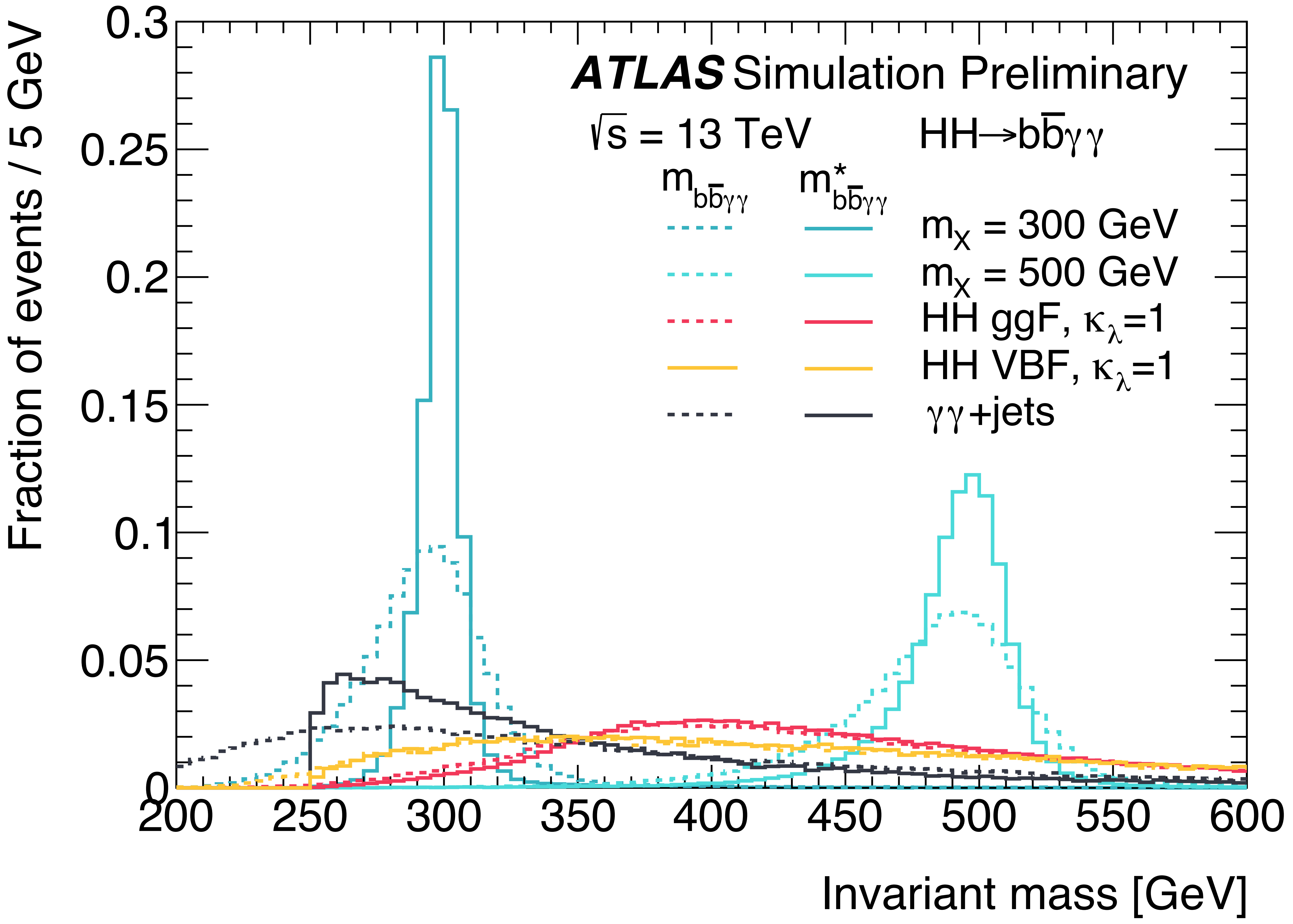

ATLAS-CONF-2021-016